

**Second measurement of seagrass and mangrove area cover
in the five Marine and Coastal Priority Protected Areas
of Phase II of the MAR Fund Project**

**Río Sarstún Multiple Use Area
Guatemala**

**Contract Services No. 002-2019 "Conservation of Marine Resources in Central
America Phase II Project" (Financial Agreement 2010 66 836)**

Final Report April 2020



RSS – Remote Sensing Solutions GmbH

Dingolfinger Straße 9
81673 Munich
Germany

www.rssgmbh.de
info@rssgmbh.de

Dr. Sandra Lohberger, Dr. Elizabeth C.
Atwood, Natalie Cornish, Dr. Claudius Mott,
Prof. Dr. Florian Siegert



Table of Contents

1	Introduction	2
2	Objectives	4
3	Project Area	4
4	Data and Methods	6
4.1	Remote Sensing Data	6
	RapidEye constellation	6
	Landsat 8	9
	Sentinel-2 constellation	12
4.2	Data Preprocessing	16
4.3	Mangrove and Seagrass Maps	17
4.4	Change Detection	21
5	Results	23
	Classification 2015	23
	Classification 2018	26
	Change analysis	31
6	Accuracy Assessment	38
7	Deliverables	42
8	Conclusions and Recommendations	43
	References	45
	Annex I	48
	Annex II	50

1 Introduction

The Mesoamerican Reef Fund (MAR Fund) was created in early 2004 to support the conservation and sustainable use of natural resources in the eco-region of the Mesoamerican Reef (MAR), shared between Belize, Guatemala, Honduras and Mexico. MAR Fund is a participatory, privately managed fund with a Board of Directors comprised of international collaborators, experts, the Central American Commission on Environment and Development (CCAD), and the in-country funds from each of the Mesoamerican Reef countries – Protected Areas Conservation Trust (Belize), Fundación para la Conservación de los Recursos Naturales y Ambiente en Guatemala (FCG), Fundación Biósfera (Honduras), and Fondo Mexicano para la Conservación de la Naturaleza (Mexico). MAR Fund’s mission is to drive regional funding and partnerships for the conservation, restoration, and sustainable use of the Mesoamerican Reef.

To accomplish these goals, MAR Fund operates as an ecoregional planning and coordinating body that prioritizes projects and allocates funding. MAR Fund aspires to be known and respected as a trustworthy and transparent fundraising mechanism able to sustain and finance effective transnational alliances, policies, and practices that conserve the Mesoamerican Reef and advance the health and well-being of the region’s people.

Implementation of the project “Conservation of Marine Resources in Central America – Phase II” is underway. This project supports best management practices, community participation in the conservation and sustainable use of coastal and marine resources in the initial network of protected areas within the Mesoamerican Reef region. Phase I and II of this project, were both funded by the German Government through the Kreditanstalt für Wiederaufbau (KfW), for a duration of five years.

As in Phase I, the current project seeks to consolidate selected protected areas in accordance with conservation priority criteria and to ensure the sustainable use of natural resources in adjacent coastal and marine areas in the medium term, in an effort to preserve the ecological functions of the Mesoamerican Reef region. The criteria for achieving these objectives, project outcomes and the assumptions underlying the objectives and results of the project are defined within the project’s Logical Framework.

The following objectives are defined for the Phase II coastal and marine protected areas (CMPAs):

1. To contribute to the conservation of the ecological functions of the Mesoamerican Reef System.
2. To consolidate selected Coastal and Marine Protected Areas (CMPA) in the project’s region and to ensure the conservation and sustainable use of marine and coastal resources in the medium term.

The following project objective indicators are listed:

Indicator 1: There is no increase in the financial gap in all of the CMPAs included in the Program.

Indicator 2: Management Plans are updated and under implementation in 100% of the CMPAs included in the Program.

Indicator 3: The CMPAs included in the Program have natural resource used plans under implementation.

The coastal and marine ecosystems within the Mesoamerican Reef region are remarkable in their biological diversity and provide a variety of ecosystem services to the adjoining nations. Ecosystem services include benefits such as shelter from tropical storms, reef fisheries, sustainment of

biodiversity, a prosperous tourism industry or the provision of building materials. Besides coral reefs, mangrove and seagrass habitats are an integral component of the coastal ecosystem.

Many studies and initiatives have proven the high potential of remote sensing techniques for assessing coastal habitats like seagrass coverage (Dekker et al. 2006, Mumby et al. 1997) or mangroves canopies (Kuenzer et al. 2011), health status and potential stress parameters in coastal ecosystems. Mapping those ecosystems via remote sensing using aerial and satellite sensors has been shown to be more cost-effective than fieldwork (Green et al. 2004, Mumby et al. 1999, Mumby et al 1997).

The following CMPAs are the main sites of investigation areas for Phase II of the project:

1. Manatee Sanctuary State Reserve, Mexico (277,452 ha)
2. Corozal Bay Wildlife Sanctuary, Belize (73,550 ha)
3. South Water Caye Marine Reserve, Belize (47,703 ha)
4. Río Sarstún Multiple Use Area, Guatemala (47,576 ha)
5. Turtle Harbour / Rock Harbour Special Marine Protection Area, Honduras (813 ha)

The outcome of this consultation is to provide the current status (2018) of seagrass and mangrove coverage in all five areas through a second measurement phase. This is followed by a comparison between the baseline (2015) and current measurement information.

The present report describes the procurement, pre-processing and classification of high resolution RapidEye, Sentinel-2 and Landsat 8 satellite imagery for the CMPA **Río Sarstún Multiple Use Area**, Guatemala.

RSS - Remote Sensing Solutions GmbH generated mangrove and seagrass cover maps that represent the 2018 cover status in the project area at a high spatial level of detail. These mangrove and seagrass cover maps provide information on different density classes and were compared to the mangrove and seagrass baseline maps from 2015. Through this comparison, it can be determined whether the two main objective indicators of the project were accomplished:

- Areas of mangroves in project CMPA equal to or greater than the baseline
- Areas of marine seagrass beds in project CMPA equal to or greater than the baseline

These two main objective indicators are impact indicators and are used to measure the overall positive impact through the implementation of the MAR Fund project.

2 Objectives

The objectives of the presented study are:

- Derivation of a reliable up-to-date (2018) coverage using actual RapidEye, Sentinel 2 and Landsat 8 satellite imagery
- Application of consistent modern classification methodologies
- Plausibility checks and accuracy assessment implemented by experts

The following information is provided:

- Mangrove area in the Río Sarstún Multiple Use Area (Guatemala) for the year 2018 – assessed at a reliable quality and comparable methodology
- Seagrass area in the Río Sarstún Multiple Use Area (Guatemala) for the year 2018 – assessed at a reliable quality and comparable methodology

3 Project Area

The Río Sarstún Multiple Use Area, was declared a protected area in 2005. The area has a size of 47,576 ha and is situated in northeast Guatemala, serving as the physical border to Belize (Figure 1). Due to its geographic location, it is considered an important protected area by both countries, with Belize also recognizing the region as a buffer zone for wetlands of the Sarstoon-Temah National Park area. Given its diversity and importance for the ecosystem landscape, the Río Sarstún wetland area was declared a RAMSAR site in 2007 (site nr. 1667). The protected area is co-administered by the National Council of Protected Areas of Guatemala together with an NGO, the Foundation for Ecodevelopment and Conservation (FUNDAECO). Within the area are located 21 communities that depend on natural resources (fishing, agriculture, and forest resources mainly) for their subsistence (Betoulle et al. 2009). Main ethnicities that contribute to the cultural wealth of the area include the Maya-Q'eqchi', the Garífunas and the Ladinos (Mojica, 2015). The complex sociocultural characteristics combined with multiple threats to its resources have required a comprehensive management approach, in which biological conservation strategies are complemented and strengthened with a participatory community model. In recent years, ecosystems threats have increased due to expanding shifting agriculture practices and slash & burn activities in pristine forests. The livestock sector is considered one of the main contributors to forest loss (Mojica, 2015). The fishing sector has had a severe impact on populations of commercial species, directly affecting artisanal fishermen and putting at risk the sustainability of marine populations subject to exploitation. Pollution flowing from the river into the sea, illegal logging and hunting, as well as oil exploitation, represent the major challenges for the conservation and sustainable management in the area.

The area consists of a river and estuarine system actively influenced by tides and sea currents, supporting mangrove forest development mainly along the eastern coast of the Río Sarstún. It is also an area of high productivity, which offers spawning, nesting, feeding and breeding areas for species of both commercial and ecological importance. The marine ecosystems of the area include patches of seagrass, mainly located to the south of where Río Sarstún flows into the ocean, and scattered coral ecosystems of great ecological importance.

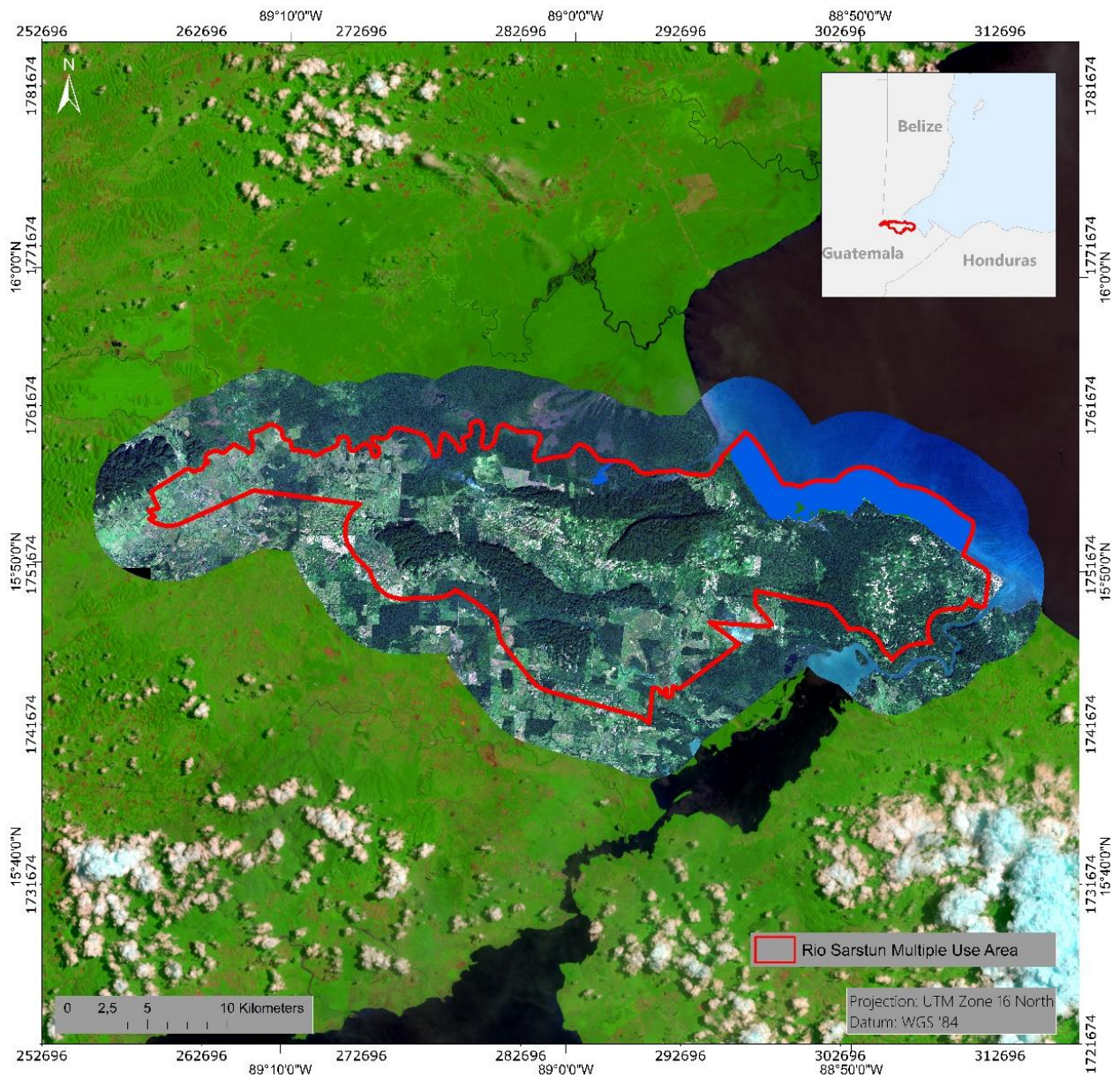


Figure 1: Overview of the Río Sarstún Multiple Use Area. True-color RapidEye imagery (2018-12-19). The border of Río Sarstún Multiple Use Area is displayed in red.

Of the coastal marine ecosystems, mangroves and seagrass meadows are considered to be among the most productive (McField and Kramer 2007; Wabnitz 2007). The main threats to the mangroves and seagrass in this area are due to: land-use change, changes in urban infrastructure, hydrological changes, anthropogenic contamination, and changing meteorological conditions (Sosa-Escalante 2013). New research on the role of vegetated coastal ecosystems has highlighted their potential as highly efficient C sinks, and led to the scientific recognition of the term "Blue Carbon" (Nellemann, 2009). Blue Carbon refers to the carbon captured by the world's coastal ocean ecosystems, mostly mangroves, salt marshes, seagrasses and potentially macroalgae. The role of Blue Carbon in climate change mitigation and adaptation has now reached international prominence (Macreadie et al., 2019).

Baseline studies of mangrove and seagrass distribution are important as damages to these ecosystems have direct and indirect negative effects on different environmental services such as: breeding areas for fish populations, reproduction, refuge, nesting, growth of different species, source of organic matter, beach stability, and sediment dynamics including capture, stabilization and formation. Seagrass meadows and mangrove forests capture and store carbon, thus protecting and restoring these coastal habitats is a good way to reduce/mitigate climate change.

Further knowledge of existence, quantity, quality, and distribution of mangroves and seagrass is indispensable to suggest adequate laws, develop strategic plans and cost / benefit assessments. Restoration measures benefit not only the environment, but also can also be designed to contribute positively the financial well-being of the local communities.

4 Data and Methods

4.1 Remote Sensing Data

Under the given framework conditions, three sources of remote sensing data were used:

RapidEye constellation

The generation of high-resolution land cover/vegetation type maps that also take different vegetation density classes into account require specific data characteristics and image analysis techniques. RSS therefore used data of the advanced satellite system constellation RapidEye, which provides high-resolution imagery within very short revisit times. The RapidEye satellite system, launched in August 2008, is a constellation of five identical satellites and thus has the unique ability to acquire high-resolution image data with 5 spectral bands on an almost daily basis (Table 1). The satellite constellation was developed by RapidEye AG and was financed with help from DLR and the state of Brandenburg. The company today belongs to Planet Labs Germany in Berlin, an offshoot of the US company Planet Labs Inc. The satellites record data with a spatial resolution of 6.5 m, which is resampled to 5 m during preprocessing by the data provider. Being able to collect more than 4 million km² of data per day as a constellation, each satellite can acquire imagery in 77 km-wide swaths extending at least 1,500 km in length. RapidEye has imaged more than 2 billion km² of Earth since February 2009.

Table 1: Characteristics of the RapidEye satellite constellation (Source: Planet Labs).

Mission Characteristics	Information	
Number of satellites	5	
Spacecraft lifetime	Over 7 years	
Orbit altitude	630 km in sun-synchronous orbit	
Equator crossing time	11:00 am local time (approximately)	
Sensor type	Multi-spectral push broom imager	
Spectral bands	Capable of capturing all of the following spectral bands:	
	<u>Band Name</u>	<u>Spectral Range (nm)</u>
	Blue	440-510
	Green	520-590
	Red	630-685
	Red edge	690-730
	NIR	760-850
Ground sampling distance (nadir)	6.5 m	
Pixel size (orthorectified)	5 m	
Swath width	77 km	

On board data storage	Up to 1,500 km of image data per orbit
Revisit time	Daily (off-nadir) / 5.5 days (at nadir)
Image capture capacity	5 million km ² /day
Camera dynamic range	12 bit

The high temporal repetition rate of RapidEye is of vital importance in regions with frequent cloud cover and short dry seasons, since it increases the probability of area coverage with acceptable cloud cover and thus makes detailed monitoring possible. RapidEye data is particularly suitable to precisely assess forest cover and forest status since their spectral, spatial, and temporal characteristics allow for a repetitive monitoring of tropical forests at high spatial detail (Figure 2).



Figure 2: Subset of a RapidEye image (true color) showing the spatial detail in land cover. The yellow rectangle in the upper right image shows the location of the subset within the Río Sarstún Multiple Use Area.

In the present study, Level 3A RapidEye imagery was used. Radiometric, sensor and geometric correction is applied to the data (Table 2). More detailed information on the data product is given in the Satellite Imagery Product Specification from Planet Labs available at:

<https://assets.planet.com/docs/combined-imagery-product-spec-april-2019.pdf> (April 2019)

Table 2: Level 3A RapidEye product specifications.

Product Attribute	Description
Product Components and Format	RapidEye Ortho image product consists of the following components: Image File – GeoTIFF file that contains image data and geolocation information Metadata File – XML format metadata file Browse Image File – GeoTIFF format Unusable Data Mask (UDM) file – GeoTIFF format
Product Orientation	Map North up
Product Framing	Image Tile (image tiles are based on a worldwide, 24km by 24km grid system). To each 24km by 24km grid square, a 500m overlap is added to produce a 25km by 25km image tile. Image tiles are black-filled 1km beyond the order polygon used during order placement. Tiles only partially covered an image take will be also black-filled in areas containing no valid image data.
Pixel Spacing	5m
Bit Depth	16-bit unsigned integers.
Product Size	Tile size is 25km (5000lines) by 25km (500 columns). 250 Mbytes per tile for 5 bands at 5m pixel spacing.
Geometric Corrections	Sensor-related effects are corrected using sensor telemetry and sensor model, bands are co-registered, and spacecraft-related effects are corrected using attitude telemetry and best available ephemeris data. Orthorectified using GCPs and fine DEMs (30m to 90m posting).
Horizontal Datum	WGS84
Map Projection	Universal Transverse Mercator (UTM)
Resampling Kernel	Cubic Convolution (default), MTF, or Nearest Neighbor

Level 3A RapidEye data from imagery 2018-12-19 was used for the mangrove and seagrass classification in Río Sarstún Multiple Use Area. Figure 3 displays this almost cloud free imagery.

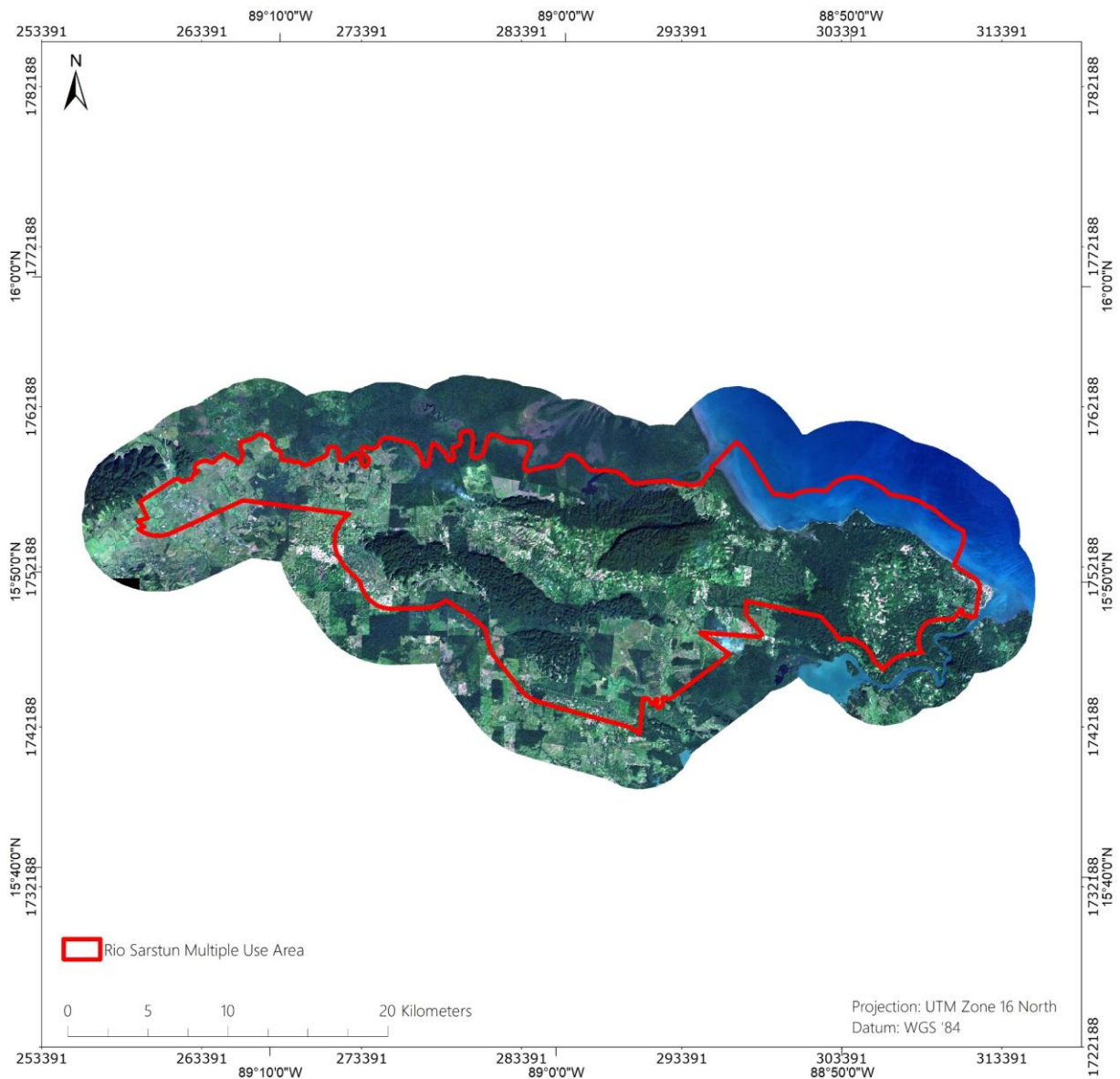


Figure 3: True-color RapidEye imagery (2018-12-19) used for mangrove and seagrass mapping.

Landsat 8

Landsat surveys the Earth's surface along the satellite's ground track in a 185-kilometer-swath as the satellite moves in a descending orbit over the sunlit side of the planet. Landsat 8 orbits the earth at 705 km altitude, crossing every point on the Earth once every 16 days. The OLI sensor onboard Landsat 8 collects data in nine shortwave bands – eight spectral bands at 30 m spatial resolution and one panchromatic band at 15 m. Refined heritage bands and the addition of a new coastal/aerosol band create data products with improved radiometric performance. OLI data products have a 16-bit range.

Table 3 gives an overview of the Landsat 8 data specifications. More detailed information on Landsat 8 data is given at: <https://www.usgs.gov/land-resources/nli/landsat/landsat-8>. Landsat 8 data is free of charge and available from the U.S. Geological Survey (USGS) agency via their ftp server: <http://earthexplorer.usgs.gov/>.

Table 3: Landsat 8 product specifications.

Product Attribute	Description
Processing	Level 1 T- Terrain Corrected
Pixel Size	OLI multispectral bands 1-7, 9: 30m OLI panchromatic band 8: 15m TIRS bands 10-11: collected at 100m but resampled to 30m to match OLI multispectral bands
Data Characteristics	<ul style="list-style-type: none"> • GeoTIFF data format • Cubic Convolution (CC) resampling • North Up (MAP) orientation • Universal Transverse Mercator (UTM) map projection (Polar Stereographic projection for scenes with a center latitude greater than or equal to -63.0 degrees) • World Geodetic System (WGS) 84 datum • 12m circular error, 90% confidence global accuracy for OLI • 41m circular error, 90% confidence global accuracy for TIRS • 16-bit pixel values

Landsat data has proven to be very appropriate for detecting forest ecosystems like mangroves (Chen et al. 2013, Kuenzer et al. 2011) (Figure 4).

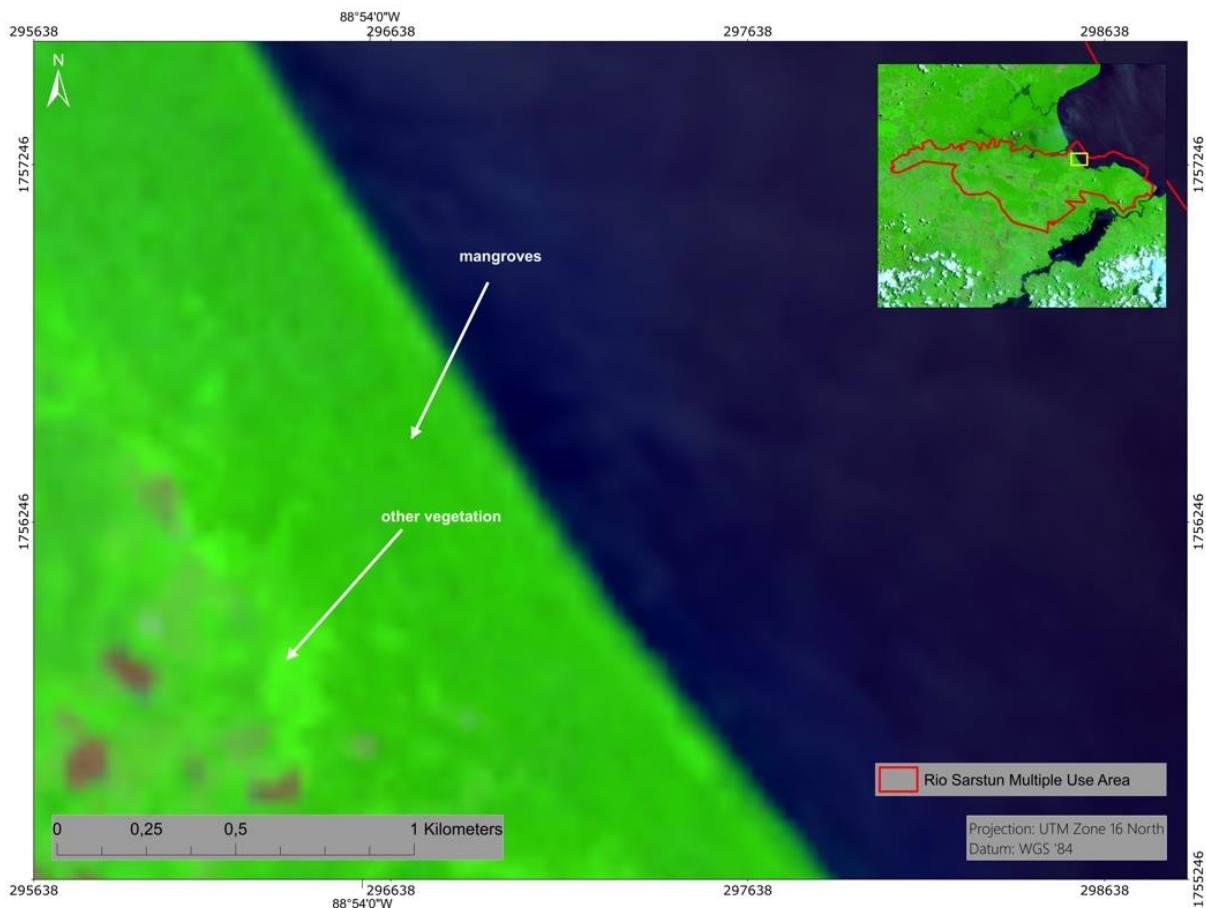


Figure 4: Subset of a Landsat 8 imagery (bands: short wavelength infrared (band 7), near infrared (band 5), and red (band 4)) showing that mangroves can be differentiated from other vegetation types. The yellow rectangle in the upper right image shows the location of the subset within the Río Sarstún Multiple Use Area.

The Landsat 8 archive was checked and the most appropriate image (2018-05-17) was downloaded. Figure 5 shows the acquired Landsat 8 data for the Río Sarstún Multiple Use Area.



Figure 5: Landsat 8 scene (2018-05-17; bands: short wavelength infrared (band 7), near infrared (band 5), and red (band 4) used for the mangrove and seagrass mapping.

Sentinel-2 constellation

The Sentinel-2 mission is based on a constellation of two satellites, both orbiting Earth at an altitude of 786 km but 180° apart. This configuration optimizes coverage and global revisit times. Sentinel-2A was launched on 23 June 2015 and Sentinel-2B was launched in March 2017. The instrument on-board the Sentinel-2 platforms is a multispectral imager (MSI) covering 13 spectral bands (443 nm – 2,190 nm) with a swath width of 290 km and a spatial resolution of 10 m (4 visible and near infrared bands), 20 m (6 red edge/short wavelength infrared bands) and 60 m (3 atmospheric bands). Table 4 gives an overview of the Sentinel-2 data specifications. More detailed information on Sentinel-2 data is provided at:

http://www.esa.int/Our_Activities/Observing_the_Earth/Copernicus/Sentinel-2.

Sentinel-2 is free of charge and available via the ESA Copernicus Open Access Hub (<https://scihub.copernicus.eu/dhus/#/home>, assessed July 2019).

Table 4: Sentinel-2 product specifications.

Sentinel-2 bands	Central wavelength (µm)	Spatial resolution (m)
Band 1 – Coastal aerosol	0.443	60
Band 2 – Blue	0.490	10
Band 3 – Green	0.560	10
Band 4 – Red	0.665	10
Band 5 – Vegetation red edge	0.705	20
Band 6 – Vegetation red edge	0.740	20
Band 7 – Vegetation red edge	0.783	20
Band 8 – NIR	0.842	10
Band 8A – Vegetation red edge	0.865	20
Band 9 – Water vapor	0.945	60
Band 10 – SWIR – cirrus	1.375	60
Band 11 – SWIR	1.610	20
Band 12 – SWIR	2.190	20

Especially due to the red-edge and short wavelength infrared bands, Sentinel-2 data has proven to be very appropriate for investigating forest ecosystems (see <https://sentinel.esa.int/web/sentinel/thematic-content/-/article/sentinels-accelerate-monitoring-of-forest-change>, November 2019), such as mangroves (Figure 6).

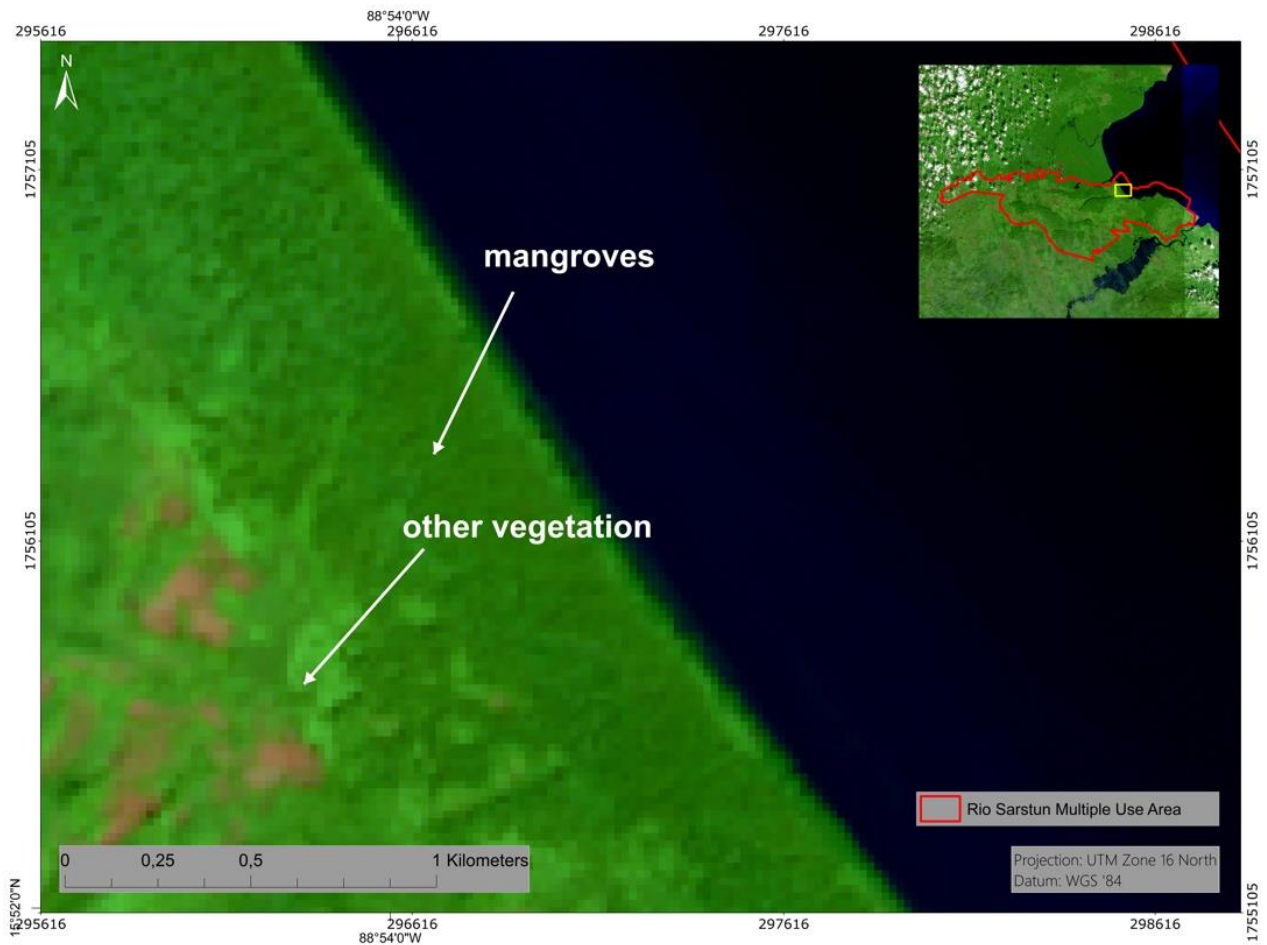


Figure 6: Subset of a Sentinel-2 imagery (2018-12-01; bands: short wavelength infrared (band 11), near infrared (band 8), and red (band 4) showing that mangroves can be differentiated from other vegetation types. The yellow rectangle in the upper right image shows the location of the subset within the Río Sarstún Multiple Use Area.

The Sentinel-2 archive was checked and the most appropriate imagery (2018-12-01, 2018-12-31) downloaded. Figure 7 shows the acquired Sentinel-2 data for the Río Sarstún test site.

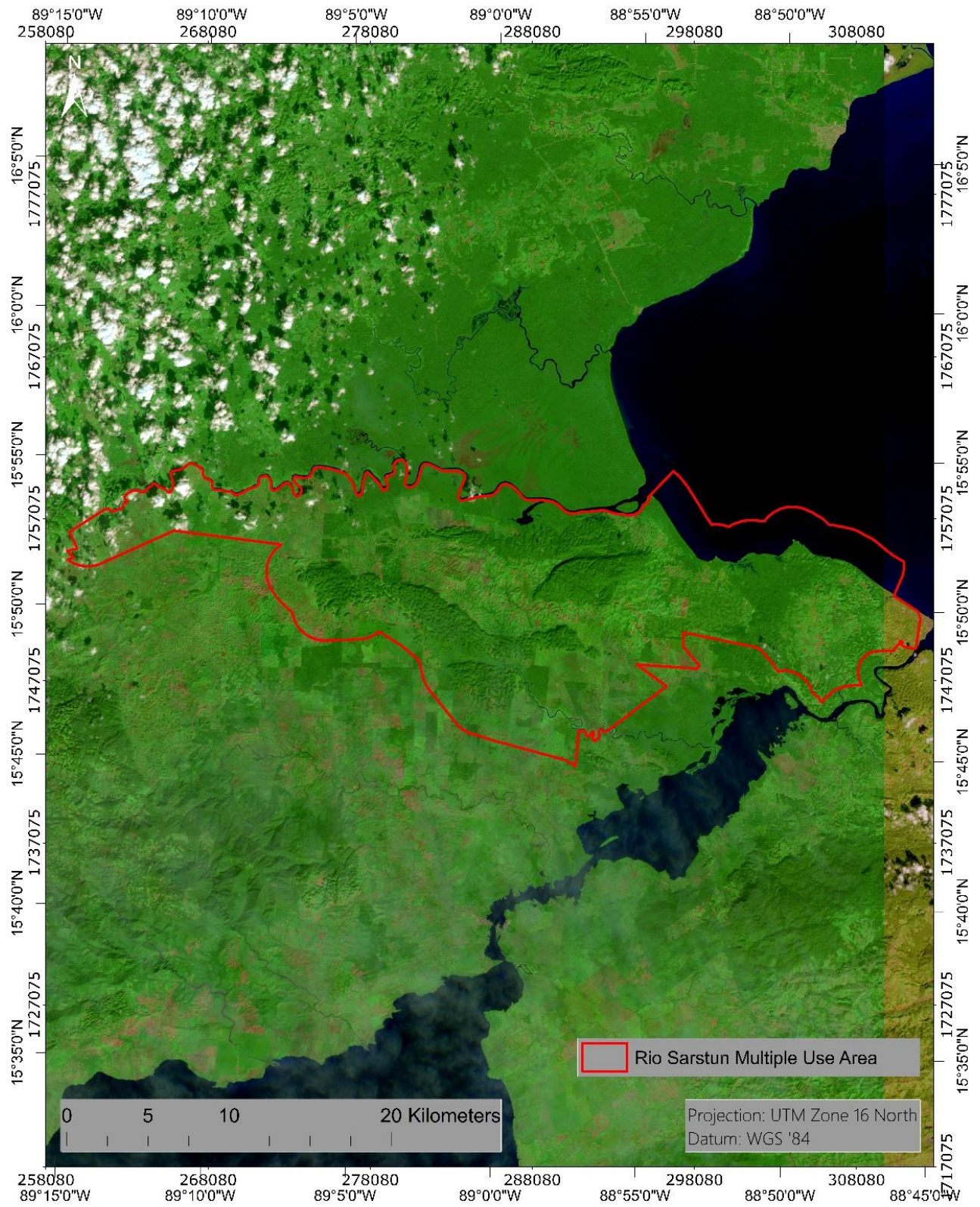


Figure 7: Sentinel-2 imagery (2018-01-12, 2018-12-31; bands: short wavelength infrared (band 11), near infrared (band 8), and red (band 4)) used for the mangrove and seagrass mapping.

4.2 Data Preprocessing

An essential preprocessing step was the removal of atmospheric effects that influence the signal, induced by water vapor and aerosols in the atmosphere as well as varying sun illumination angles in different seasons. This preprocessing step results in the calibration of the data and allows an estimation of the surface reflectance without atmospheric distortion effects. The calibration method facilitates an improved scene-to-scene radiometric measurements comparability, which is a necessary precondition for the subsequent semi-automatic object-based rule-set classification method.

Atmospheric correction of Sentinel-2 data

Sentinel-2 data was corrected with Sen2Cor, a processor published by ESA (<https://step.esa.int/main/third-party-plugins-2/sen2cor/>). Sen2Cor is a processor for Sentinel-2 Level 2A product generation and formatting; it performs the atmospheric-, terrain and cirrus correction of Top-Of- Atmosphere Level 1C input data. Sen2Cor creates Bottom-Of-Atmosphere, optionally terrain- and cirrus corrected reflectance images; additional, Aerosol Optical Thickness-, Water Vapor-, Scene Classification Maps and Quality Indicators for cloud and snow probabilities. Its output product format is equivalent to the Level 1C User Product: JPEG 2000 images, three different resolutions, 60, 20 and 10 m.

Atmospheric correction of Landsat 8

Landsat 8 data were corrected using ARCSI (<https://www.arcsi.remotesensing.info/>, July 2019). ARCSI is a software that provides a command line tool for the generation of Analysis Ready Data optical data including atmospheric correction, cloud masking, topographic correction etc. of Earth Observation optical imagery (Blue-SWIR).

Landsat 8 product specifications state that the OLI has a geolocation uncertainty of less than 12 m circular error. Visual analysis showed that the Sentinel-2 and Landsat 8 data had an excellent geometrical fit with the RapidEye data so no geometrical co-registration was necessary.

Atmospheric correction of RapidEye

RapidEye imagery was corrected with ATCOR-2 (Richter and Schläpfer 2011; http://www.rese.ch/products/atcor/atcor3/atcor2_method.html). The following parameters were used in ATCOR-2:

- Atm. Correction: pre-defined sensors, flat terrain
- Acquisition date of the satellite data
- Selection of sensor (RapidEye) and corresponding calibration file
- Atmospheric file: tropical maritime
- Satellite and sun geometry from the metadata of the satellite data
- Ground elevation: 0 km

4.3 Mangrove and Seagrass Maps

The basic classification method was an object-based image analysis approach using eCognition software (Trimble Geospatial, Munich, Germany). This methodology classifies spatially adjacent and spectrally similar groups of pixels, so called image objects, rather than individual pixels of the image. Traditional pixel-based classification uses multi-spectral classification techniques that assign a pixel to a class by considering the spectral similarities with the class or with other classes. The resulting thematic classifications are often incomplete and non-homogeneous. The received signal frequency does not clearly indicate the membership to a land cover class, e.g. due to atmospheric scattering, mixed pixels, or the heterogeneity of natural land cover. Improvements in the spatial resolution of remote sensing systems employed results in increased complexity of the data. The representation of real-world objects in the feature space is characterized by high variance of pixel values, hence statistical classification routines based on the spectral dimensions are limited and a greater emphasis must be placed on exploiting spatial and contextual attributes (Guindon 1997, Guindon 2000, Matsuyama 1987). To enhance classification, the use of spatial information inherent in such data was proposed and studied by many researchers (Atkinson and Lewis 2000). A lot of approaches make use of the spatial dependence of adjacent pixels. Approved routines are the inclusion of texture information, the analysis of the (semi-)variogram, or region growing algorithms that evaluate the spectral resemblance of proximate pixels (Hay et al. 1996, Kartikeyan et al. 1998, Woodcock et al. 1988). In this context, the use of object-oriented classification methods on remote sensing data has gained immense popularity, and the idea behind it was subject to numerous investigations since the 1970's (Haralick and Joo 1986, Kartikeyan et al. 1995, Kettig and Landgrebe 1976)

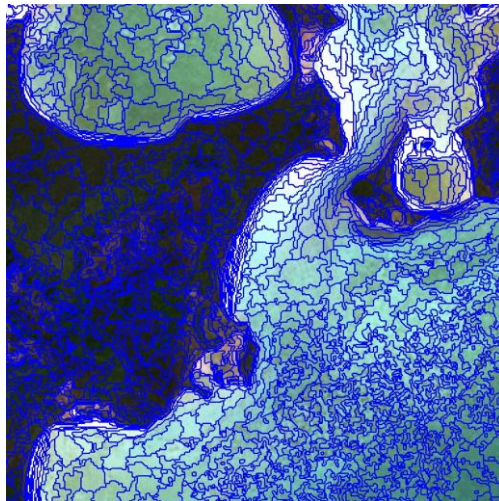
In the object-oriented approach in a first step a segmentation of the imagery generates image objects, combining neighboring pixel clusters to an image object. Here the spectral reflectance, as well as texture information and shape indicators are analyzed for generating the objects. The attributes of the image objects like spectral reflectance, texture or NDVI are stored in a so-called object database (Benz 2004, Mott 2005). Classification itself corresponds in fact to a complex database query by formulating rule bases on how the object attributes should be evaluated. Additionally, expert knowledge can be implemented in the classification process.

This approach consists of three basic procedures (depicted in Figure 8):

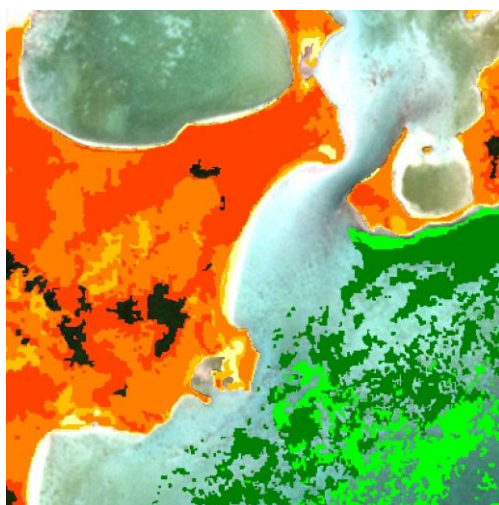
- **Design of a class hierarchy:** Definition of classes and inheritance rules between parent and child classes
- **Image segmentation:** The input image raster dataset is segmented into homogeneous image objects according to their spectral and textural characteristics
- **Classification:** The image objects are assigned to the predefined classes according to decision rules which can be based on spectral, spatial, geometric, thematic or topologic criteria



(a) RapidEye satellite image



(b) Image segmentation



- Mangrove 0-25%
- Mangrove 25-50%
- Mangrove 50-75%
- Mangrove 75-100%
- Seagrass 20-50%
- Seagrass 50-100%

(c) Classification based on image object attributes

Figure 8: Example of the basic procedures of an object object-based image analysis. The input satellite imagery (a) is first segmented into homogeneous image objects (b) and then assigned to predefined classes using decision rules (c).

A total of seven ecological classes were defined for this project:

4 mangrove density classes:

1. 0-25%
2. 25-50%
3. 50-75%
4. 75-100%

3 aquatic classes:

1. Water, including 0-20% seagrass coverage
2. 20-50% seagrass coverage
3. 50-100% seagrass coverage

In keeping with the results from the 2015 baseline analysis of Río Sarstún Multiple Use Area, the originally proposed classification scheme stratifying 25% levels of coverage was not possible to implement while keeping with reliable scientific standards. Due to turbidity of the ocean, especially in shallow waters, very low seagrass coverages may not be reliably detected. Turbidity, caused by high concentrations of suspended matter in shallow waters, makes a reliable detection of isolated seagrass patches difficult. Total suspended matter can include a wide variety of material, such as silt, decaying plant and animal matter, industrial waste as well as sewage (Figure 9).

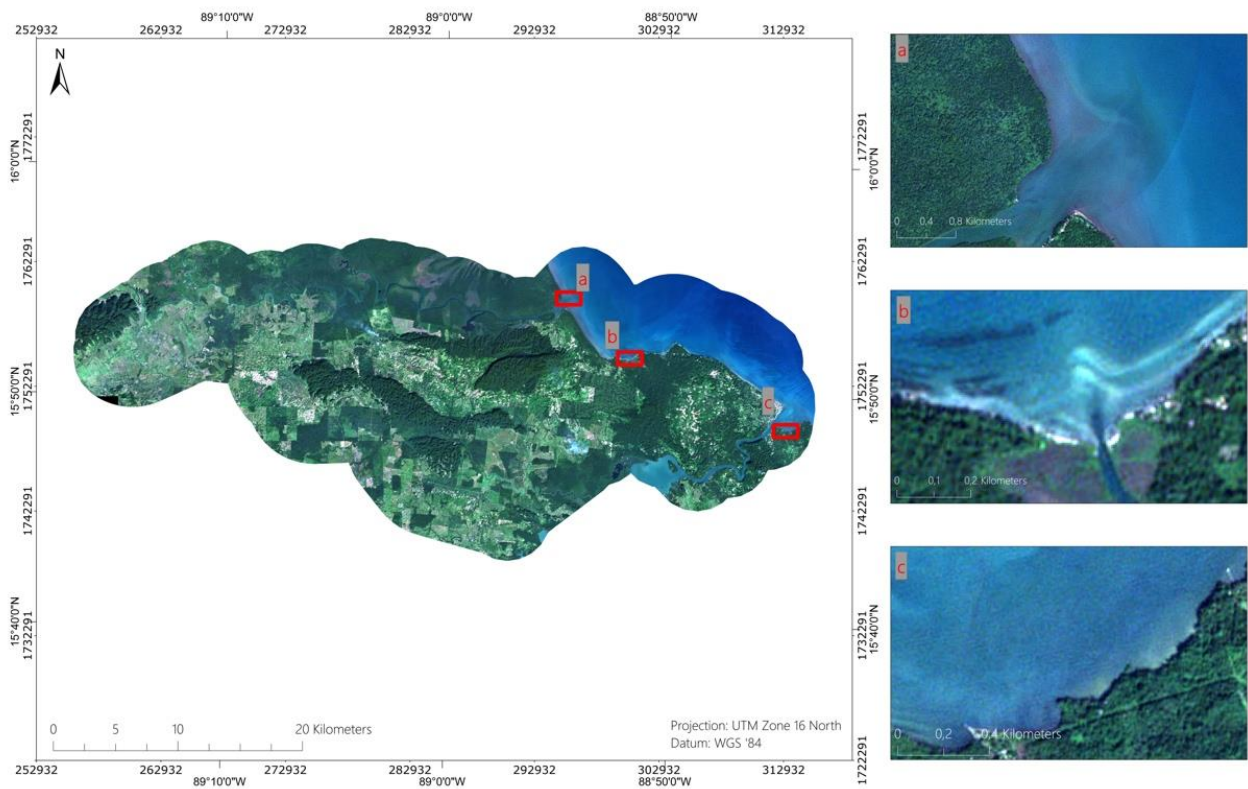


Figure 9: Examples for strong turbid sea within the project area. Here it was not possible to detect 4 density classes for seagrass. True-color RapidEye imagery (2018-12-19).

The classification scheme concerning aquatic habitats was adjusted to the same three classes used in the 2015 baseline study: Water including 0-20% seagrass coverage, 20-50% and 50-100% seagrass coverage.

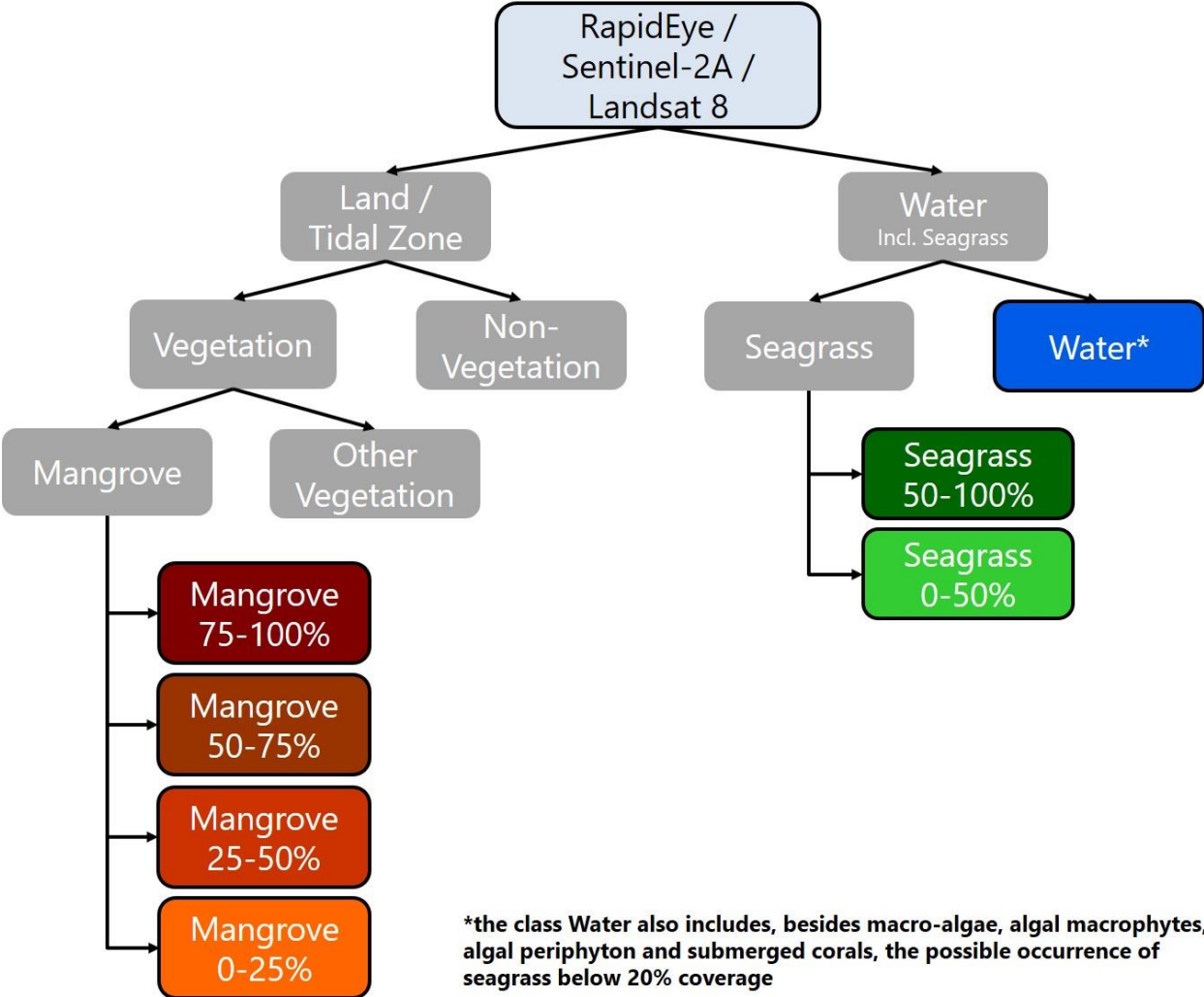


Figure 10: Classification scheme of the mangrove and seagrass cover classification of the Río Sarstún Multiple Use Area. Grey boxes without frame represent parent classes, framed boxes represent the final classes with the associated color from the land cover maps (Figures 10-11 and 14-15). It is important to notice that the class Water also includes, besides macro-algae, algal macrophytes, algal periphyton and submerged coral, the possible occurrence of seagrass below 20% coverage.

The RapidEye image mosaic was segmented into objects of adjacent, spectrally similar pixels by the multi-resolution segmentation algorithm implemented in eCognition, and subsequently classified according to the classification scheme shown in Figure 10. The classification rule-set works in a hierarchical manner from coarse to fine thematic details. On the first hierarchy level, discrimination between Land / Tidal Zone areas and Water areas (incl. seagrass) was conducted based on spectral thresholds. On the next level of the hierarchy, all Land / Tidal Zone objects were discriminated into Vegetation and Non-Vegetation objects according to their spectral properties. Water was discriminated into Seagrass and Water. On the third hierarchy level the vegetated objects were distinguished into Mangrove and Other Vegetation according to their spectral properties.

The analyses showed that the spatial and spectral resolution of the RapidEye satellite data does not allow for seagrass to be detected unambiguously below 20% coverage. As a result, the class water includes macroalgae, algal macrophytes, algal periphyton and submerged corals, as well as the possible occurrence of seagrass below 20% coverage. Mangroves were further distinguished into 4 density classes (75-100%, 50-75%, 25-50%, and 20-25%) and seagrass into two density classes (50-100% and 20-50%) based on spectral and texture properties, as well as visual interpretation of the imagery. After the object-oriented classification, an intensive visual revision by a trained expert was conducted. The results are georeferenced shp-files ready to be used in a geographic information system, like ArcGIS. XML-Metadata was generated for all deliverables. Annex I gives an overview of the segmentation parameters and spectral bands used in the baseline classification. Further the statistical parameters of the feature objects for the different classes are shown.

4.4 Change Detection

In order to assess the changes in the Rio Sarstun area of the recent years, we compared the up-to-date mangrove and seagrass maps (2018) with the ones derived for the year 2015 baseline (Ballhorn et al. 2016): a change detection analysis was conducted. In ArcGIS, the resulting mangrove and seagrass maps of the two classifications (2015 and 2018) were intersected in order to derive areas of change. Figure 11 schematically displays the workflow of this post-classification change detection process. Our approach is a quantitative and qualitative comparison of two classifications (baseline, 2015 and final measurement, 2018).

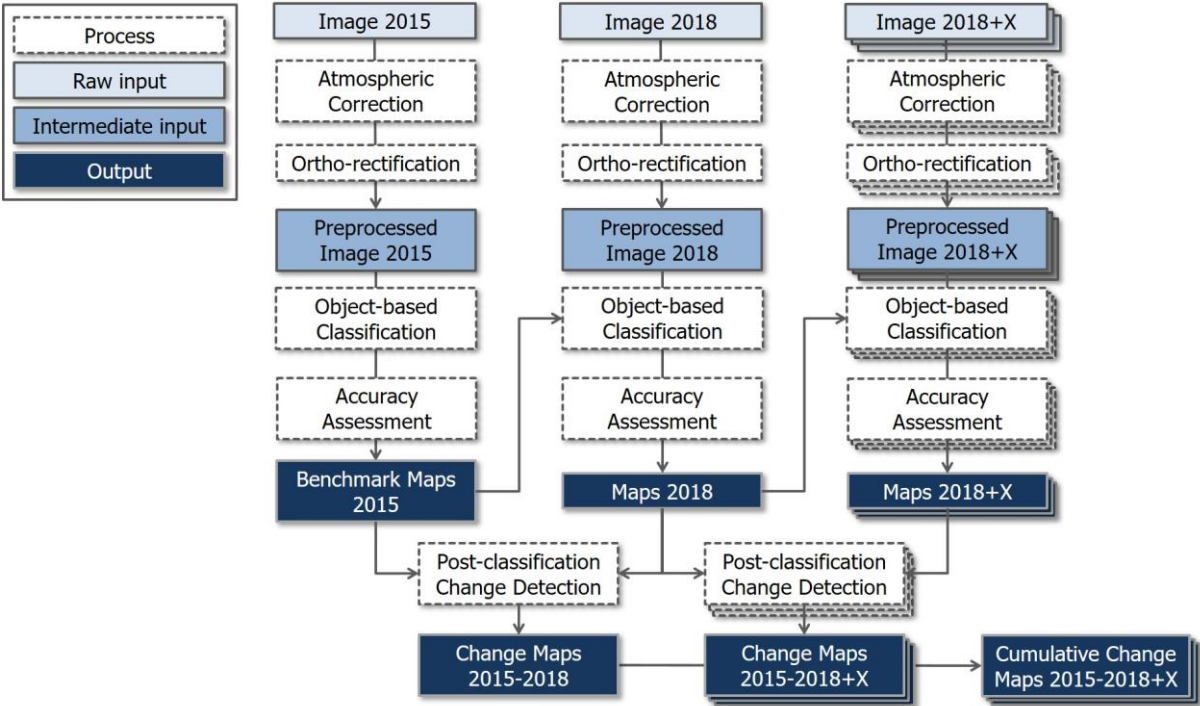


Figure 11: Schematic representation of the post-classification change detection process in order to analyze changes in mangrove and seagrass cover between the two classifications (baseline, 2015 and final measurement, 2018).

Monitoring techniques based on multispectral satellite-acquired data have demonstrated potential as a means to detect, identify, and map changes in forest cover (Coppin 2004) and seagrass (Misvari and Hashim 2016).

5 Results

Figure 14 and Figure 15 show the results for the final measurement of mangrove and seagrass cover classification. The overview maps are provided as high-resolution pdfs that may be printed in A0 and displayed at an enlarged scale on a desktop computer. Comparable thematic maps reflecting the status of mangrove and seagrass cover in 2015 were provided during the baseline study (see report Ballhorn et al. 2016).

The highest image resolution of the data we analyze in this study is the RapidEye imagery. The spatial resolution of RapidEye imagery is 6.5 m, resampled to 5 m (resampled by the data provider). Being the dataset with the highest resolution, it defines the MMU (minimum mapping unit). It is the specific size of the smallest feature that is being reliably mapped in a study. The MMU can be defined by 3x3 pixels, which means would mean $(6.5\text{m} \times 3) \times (6.5\text{m} \times 3) = 380,25\text{m}^2$. This only allows to generate an accuracy in this scale, meaning that any results in hectares may only be given with an accuracy of the first decimal after the dot (corresponding 1.000m^2).

Baseline Classification (2015)

Table 5 gives an overview of the remote sensing data used for the mangrove and seagrass classification during the baseline measurement in year 2015. Images with different acquisition dates within the year 2015 were used to get a preferably cloud free coverage of the study area.

Table 5: Overview of remote sensing data used for the mangrove and seagrass classification during the baseline measurement in 2015.

Rapid Eye		
Amount tiles	Acquisition date	Cloud cover within study area (%)
7 (level 3A)	2015-04-27	10
1 (level 3A)	2015-10-31	0
Landsat 8		
Amount images	Acquisition date	Cloud cover within study area (%)
1	2014-02-28	10

Figure 12 and Figure 13 show the results for the mangrove and seagrass cover classification for the baseline completed in 2015.

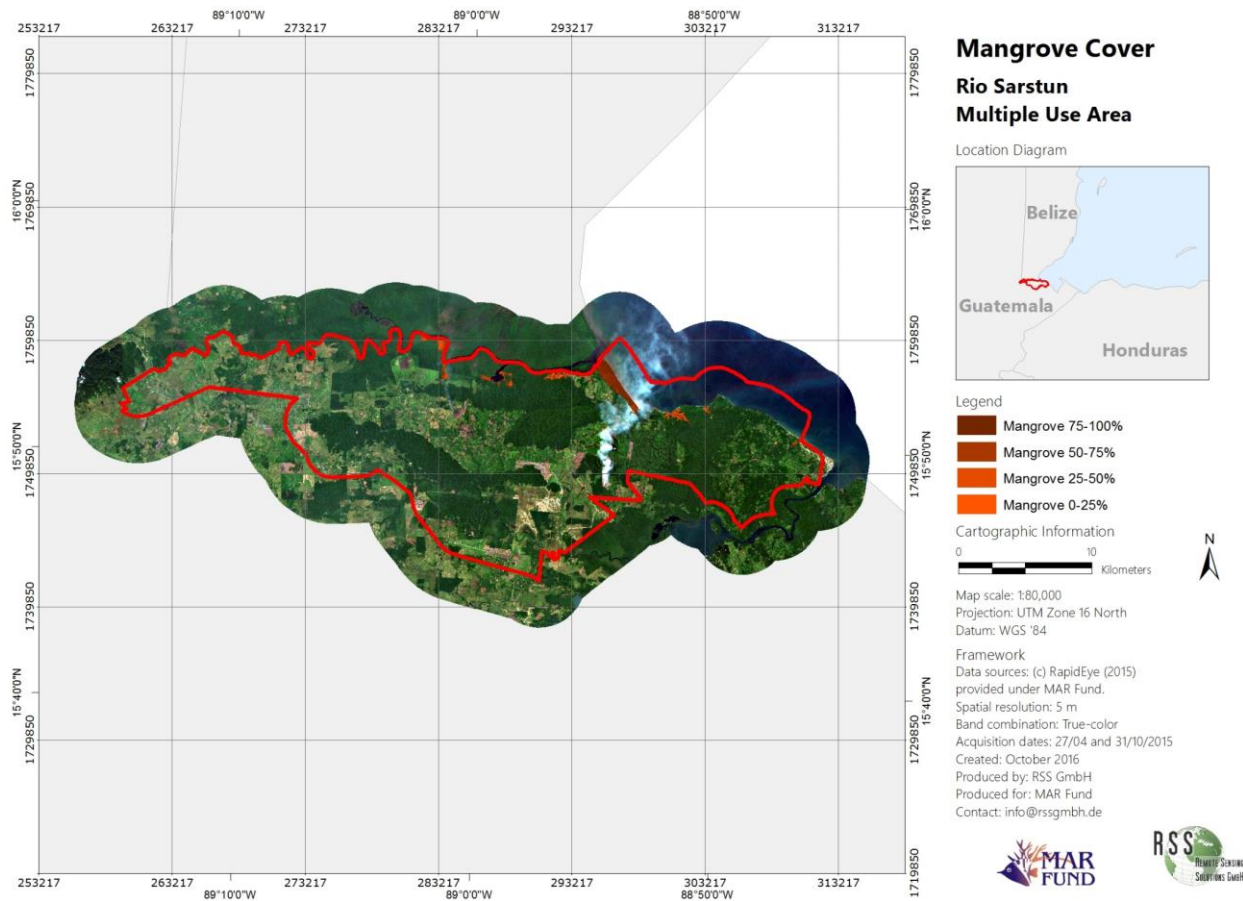


Figure 12: Mangrove cover classification for the Río Sarstún Multiple Use Area from 2015. The four mangrove density classes (0-25%, 25-50%, 50-75%, and 75-100%) are shown over RapidEye imagery from 2015. In the upper right diagram, the location of the Río Sarstún Multiple Use Area within Guatemala is displayed (red).

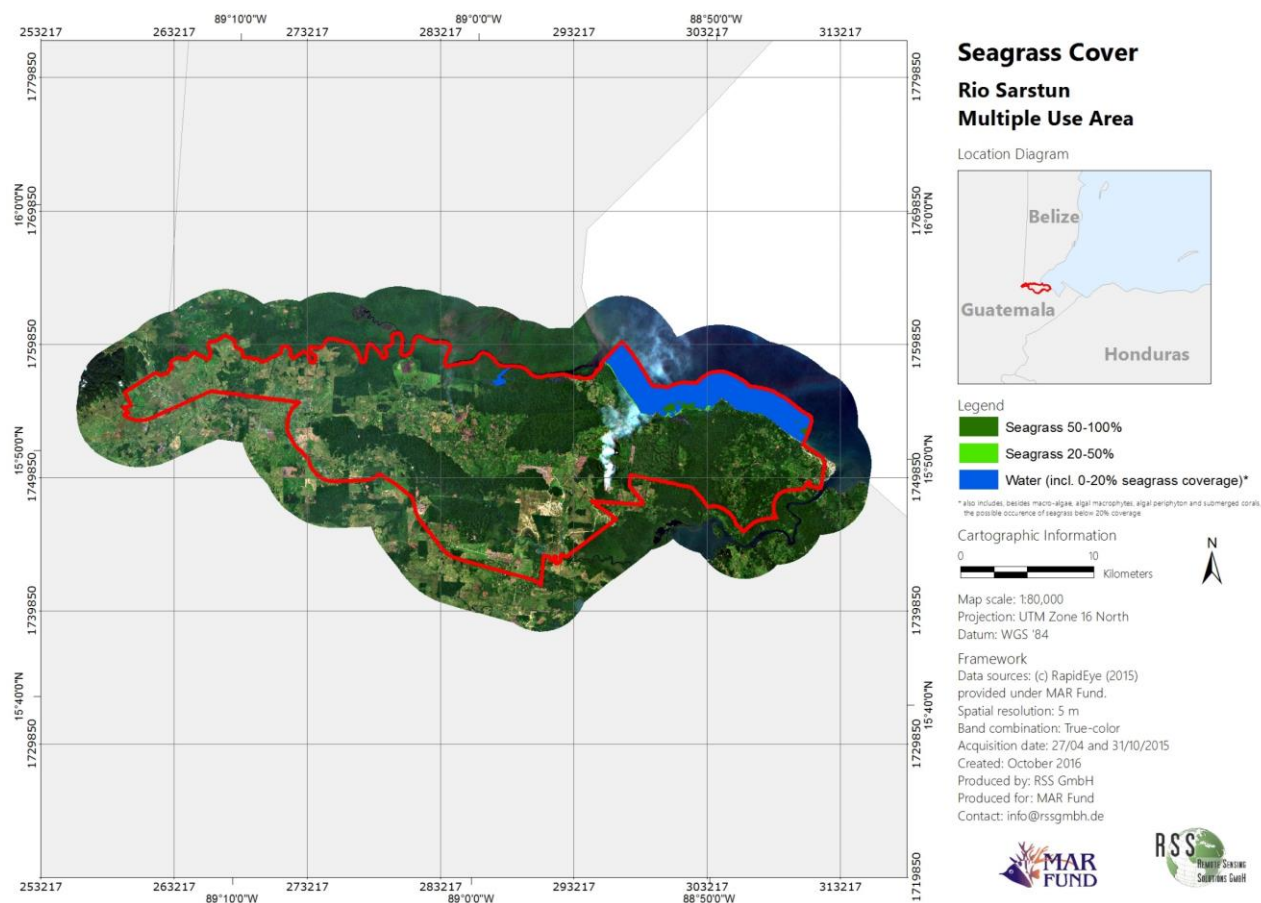


Figure 13: Seagrass cover classification for the Río Sarstún Multiple Use Area from 2015. The three aquatic classes (Water incl. 0-20% seagrass coverage, 20-50%, and 50-100% seagrass coverage) are shown over RapidEye imagery from 2015. In the upper right diagram, the location of the Río Sarstún Multiple Use Area within Guatemala is displayed (red).

Table 6 displays the spatial extent of the mangrove and seagrass classes completed for the baseline in 2015 (see Ballhorn et al. 2016).

Table 6: Spatial extent of the different ecological classes classified for the baseline in 2015 in the Río Sarstún Multiple Use Area. Also shown are the percentage of the total mangrove/seagrass cover and the percentage of the total Río Sarstún Multiple Use Area, area for each class.

Ecological Class	Area (ha)	Percentage of total mangrove/seagrass cover (%)	Percentage of total study area (47,576 ha) (%)
Mangrove 75-100%	250.5	38.5	0.5
Mangrove 50-75%	216.3	33.3	0.5
Mangrove 25-50%	103.6	15.9	0.2
Mangrove 0-25%	80.0	12.3	0.2
Sum Mangrove	650.5	100.0	1.4
Seagrass 50-100%	125.4	65.7	0.3
Seagrass 20-50%	65.5	34.3	0.1
Sum Seagrass	190.9	100.0	0.4

Final Classification 2018

Table 7 gives an overview of the remote sensing data used for the mangrove and seagrass classification during the final measurement in year 2018. Images with different acquisition dates within the year were used to get a preferably cloud free coverage of the study area.

Table 7: Overview of remote sensing data used for the final measurement of mangrove and seagrass classification of the year 2018.

Rapid Eye		
Amount tiles	Acquisition date	Cloud cover within study area (%)
7 (level 3A)	2018-12-19	0
Sentinel-2		
Amount images	Acquisition date	Cloud cover within study area (%)
1	2018-12-01	5
1	2018-12-31	10
Landsat 8		
Amount images	Acquisition date	Cloud cover within study area (%)
1	2018-05-17	<1

Figure 14 and Figure 15 show the results for the final measurement (2018) for mangrove and seagrass cover classification.

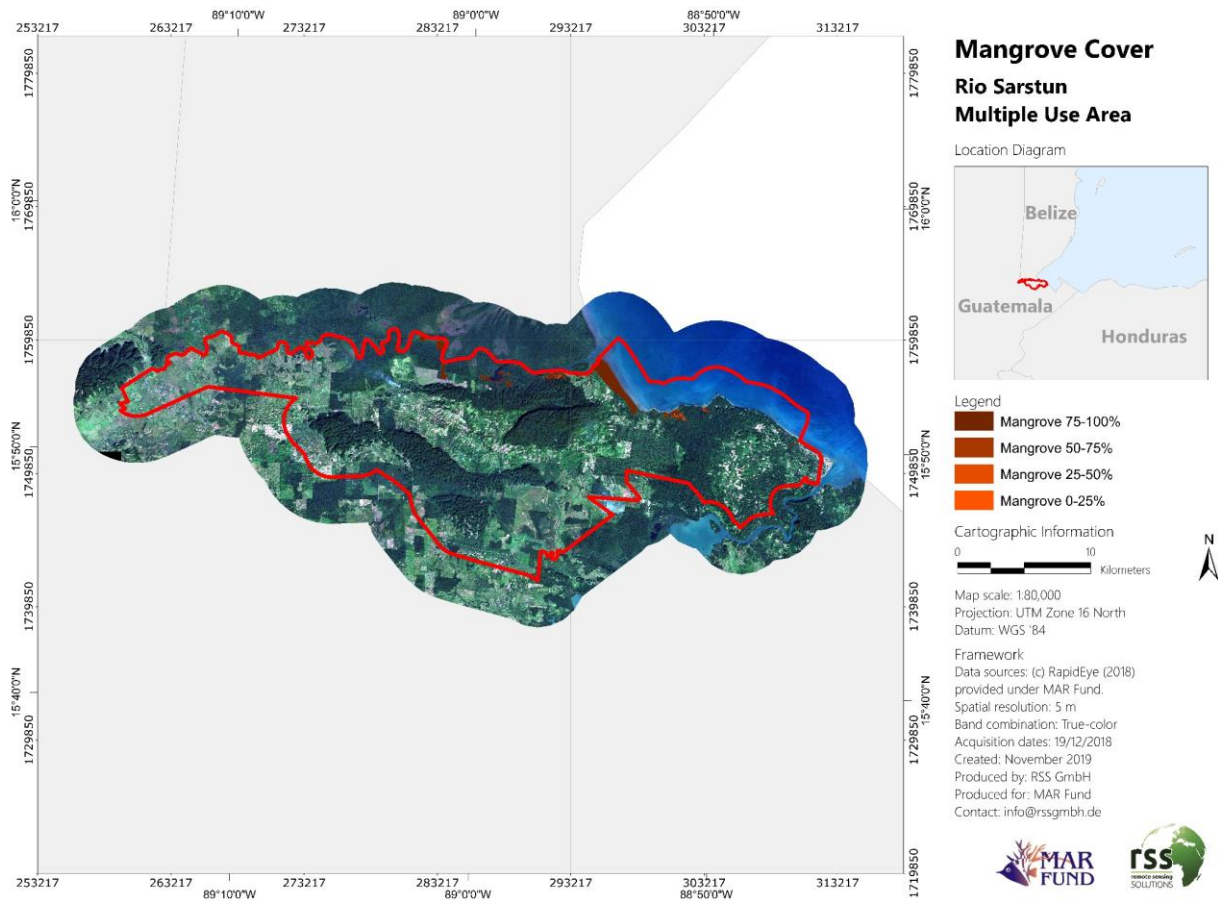


Figure 14: Mangrove cover classification for the Río Sarstún Multiple Use Area from 2018. The four mangrove density classes (0-25%, 25-50%, 50-75%, and 75-100%) are shown over RapidEye imagery from 2018. In the upper right diagram, the location of the Río Sarstún Multiple Use Area within Guatemala is displayed (red).

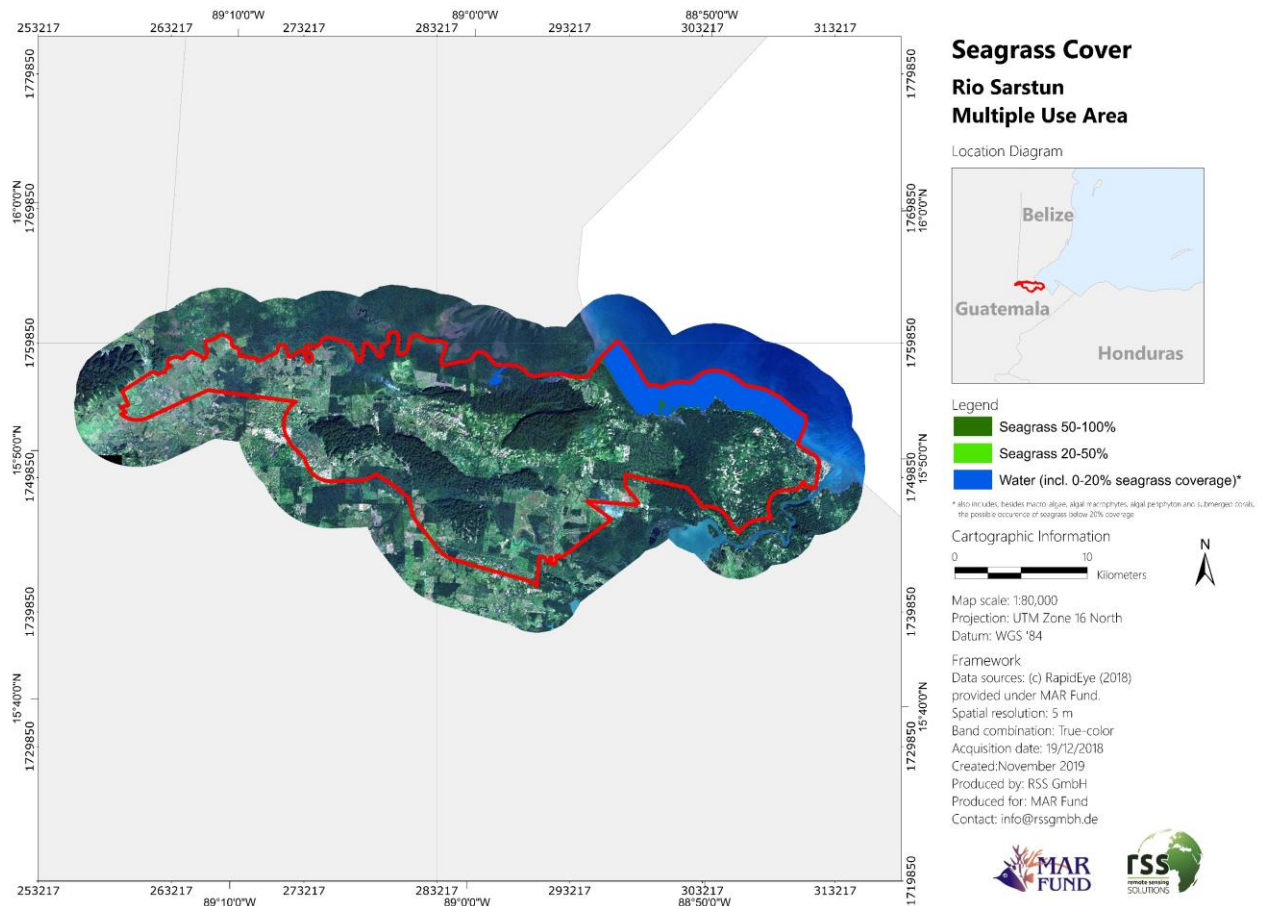


Figure 15: Seagrass cover classification for the Río Sarstún Multiple Use Area 2018. The three aquatic classes (Water incl. 0-20% seagrass coverage, 20-50%, and 50-100% seagrass coverage) are shown over RapidEye imagery from 2018. In the upper right diagram, the location of the Río Sarstún Multiple Use Area within Guatemala is displayed (red).

Table 8 displays the spatial extent of these different mangrove and seagrass classes for the year 2018.

Table 8: Spatial extent of the different ecological classes classified for the year 2018 in the Río Sarstún Multiple Use Area. Also shown are the percentage of the total mangrove/seagrass cover and the percentage of the total Río Sarstún Multiple Use Area, area for each class.

Ecological Class	Area (ha)	Percentage of total mangrove/seagrass cover (%)	Percentage of total study area (47,576 ha) (%)
Mangrove 75-100%	581.5	89.9	1.2
Mangrove 50-75%	42.9	6.6	0.1
Mangrove 25-50%	14.2	2.2	0.0
Mangrove 0-25%	8.4	1.3	0.0
Sum Mangrove	647.0	100.0	1.4
Seagrass 50-100%	96.2	87.9	0.2
Seagrass 20-50%	13.2	12.1	0.0
Sum Seagrass	109.4	100.0	0.2

The graphs in Figure 16 and Figure 17 display the spatial extent of the ecological classes classified within the Río Sarstún Multiple Use Area for the final measurement in 2018. The chart colors correspond to the class colors in the final maps (Figures 12 &14 and 13 & 15).

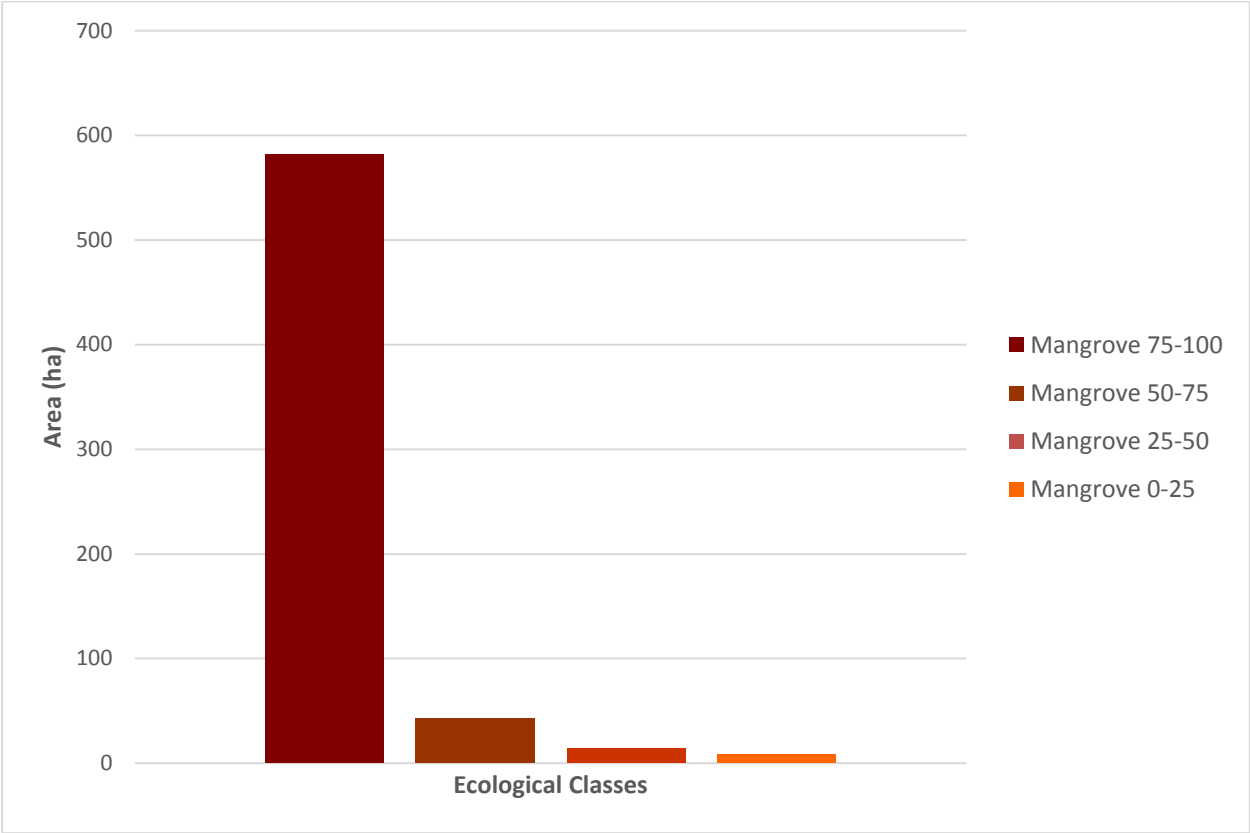


Figure 16: Spatial extent of the different mangrove density classes within the Río Sarstún Multiple Use Area from the final measurement in 2018. Colors correspond to those used in Figures 12 & 14.

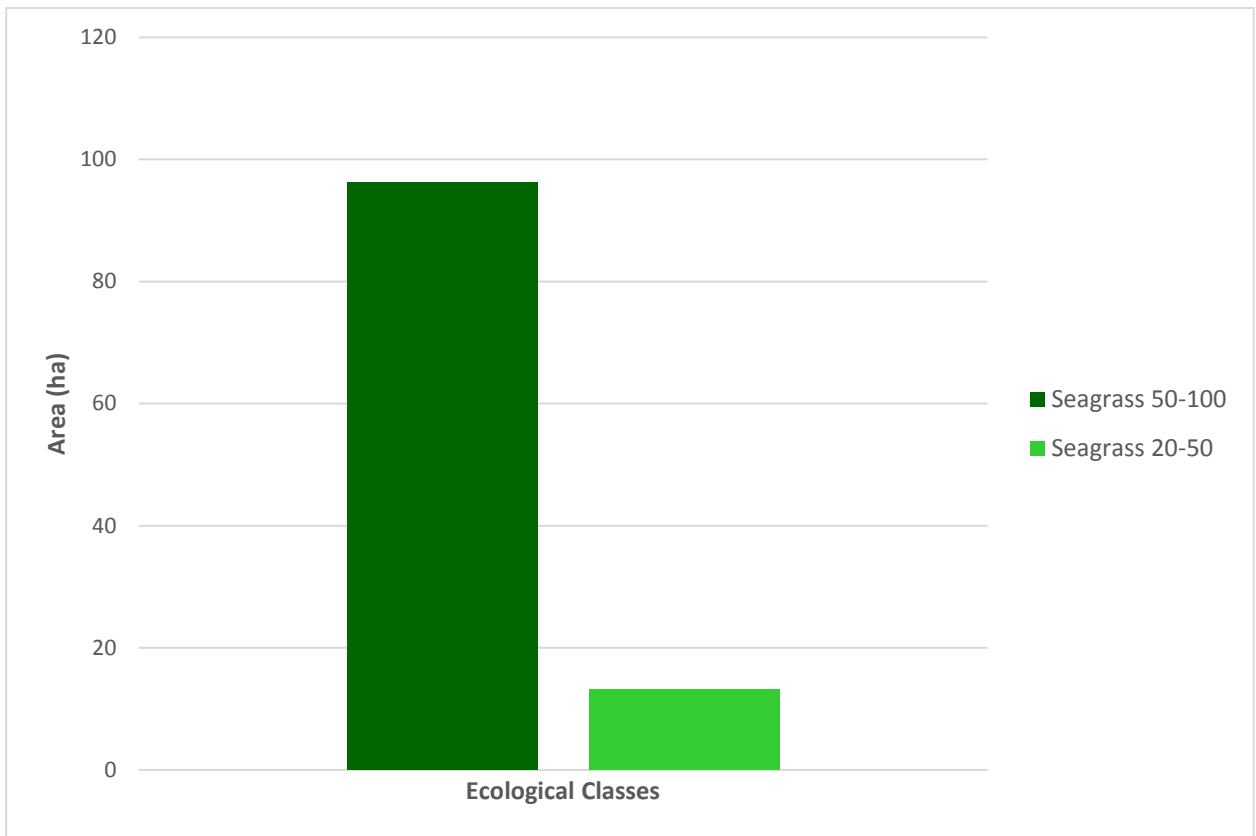


Figure 17: Spatial extent of the different seagrass density classes within the R o Sarst n Multiple Use Area from the final measurement in 2018. Colors correspond to those used in Figures 13 & 15.

Change analysis

Total mangrove cover and total seagrass cover were recorded to measure the changes between the baseline done in 2015 and the final measurement done in 2018.

Table 9: Combined overview of respective class areas between the baseline and final measurement, as taken from Table 6 and Table 8.

Ecological Class	Area (ha)		Percentage of total mangrove/seagrass cover (%)		Percentage of total study area (%)	
	2015	2018	2015	2018	2015	2018
Mangrove 75-100%	250.5	581.5	38.5	89.9	0.5	1.2
Mangrove 50-75%	216.3	42.9	33.3	6.6	0.5	0.1
Mangrove 25-50%	103.6	14.2	15.9	2.2	0.2	0.0
Mangrove 0-25%	80.0	8.4	12.3	1.3	0.2	0.0
Sum Mangrove	650.5	647.0	100.0	100.0	1.4	1.4
Seagrass 50-100%	125.4	96.2	65.7	87.9	0.3	0.2
Seagrass 20-50%	65.5	13.2	34.3	12.1	0.1	0.0
Sum Seagrass	190.9	109.4	100.0	100.0	0.4	0.2

Table 10: Total change between the baseline (2015) and final measurement (2018), provided in hectares, the percent change within all mangrove or seagrass classes, and percent change within the total study area. Please note that these are rounded values.

Ecological Class	Change in area (ha)	Change within total mangrove/seagrass cover (%)	Change in total study area (%)
Mangrove 75-100%	331.0	51.2	0.7
Mangrove 50-75%	-173.4	-26.8	-0.4
Mangrove 25-50%	-89.4	-13.8	-0.2
Mangrove 0-25%	-71.6	-11.1	-0.2
Sum Mangrove	-3.4	-0.5	0.0
Seagrass 50-100%	-29.2	-26.7	-0.1
Seagrass 20-50%	-52.3	-47.8	-0.1
Sum Seagrass	-81.5	-74.5	-0.2

The largest change is reflected in the densest mangrove class (Table 10). Mangrove 75-100% saw an increase in area of 331.0 ha, while all other classes decreased by less than half of this amount.

A more detailed assessment of the overall class changes between these two measurements can be seen in Table 11.

Table 11: Detailed change matrix of the different land covers between the baseline (2015) and the final measurement (2018), provided in hectares (ha). These values were generated by intersecting the classifications of 2015 and 2018. The results of the intersection are displayed in a correspondence matrix, which is the de facto method for reporting land cover changes over two time periods. The table should be read horizontally (from left to right) for the land cover detected in 2015 and vertically (top to bottom) for the assessed land cover of the year 2018. The different colors of the cells represent whether no change, loss, degradation or regeneration occurred within the mangrove or seagrass classes. The legend at the bottom of the table displays, which color represents which change process. Congalton (1991) describes the background of accuracy assessment of remote sensing imagery and set standards in accuracy assessment methodology.

		Classification 2018 (ha)								Sum
		Land / Tidal Zone	Mangrove 0-25	Mangrove 25-50	Mangrove 50-75	Mangrove 75-100	Seagrass 20-50	Seagrass 50-100	Water	
Classification 2015	Land / Tidal Zone	43,130.5	0.0		0.0	1.5	3.8	1.0	13.8	43,150.6
	Mangrove 0-25	0.2	7.5	13.3	36.2	22.8			0.0	80.0
	Mangrove 25-50	0.6	0.7	0.6	6.1	95.4			0.2	103.6
	Mangrove 50-75	3.2	0.2	0.2	0.2	211.9			0.6	216.3
	Mangrove 75-100	0.1		0.1	0.4	249.8				250.4
	Seagrass 20-50	4.4					0.5	21.1	39.5	65.5
	Seagrass 50-100						7.3	28.1	90.1	125.5
	Water						1.6	46.0	3,536.7	3,584.3
	Sum	43,139.0	8.4	14.2	42.9	581.4	13.2	96.2	3,680.9	47,576.2
	No Change									
	Loss/Deforestation									
	Degradation									
	Gain/Reforestation									
	Regeneration									

Table 12 summarizes the categorical changes recorded between the baseline (2015) and the current observed cover (2018). Deforestation (or loss) is defined as the change of one of the density classes (either mangrove or seagrass) to a non density class (water or land/tidal zone). Degradation is the change of a density classes (mangrove or seagrass) to a lower density class of the same land cover. Reforestation (or gain) is the change from a non density class (water or land/tidal zone) to a density class of either mangrove or seagrass. Regeneration is the change of a lower density class (either mangrove or seagrass) to a higher density class. Mangrove reforestation and regeneration is clearly proven between the baseline (2015) and final measurement (2018). The trend observed for seagrass is discussed in more detail below.

Table 12: Summarized changes between the baseline (2015) and final measurement (2018) in hectare (ha).

Change Class	Area (ha)
Mangrove Deforestation	4.9
Mangrove Degradation	1.6
Mangrove Reforestation	1.5
Mangrove Regeneration	372.4
Seagrass Loss	94.5
Seagrass Degradation	7.3
Seagrass Gain	52.4
Seagrass Regeneration	21.1
Seagrass to Mangrove	0.0
Mangrove to Seagrass	0.0
Land / Tidal Zone to Water	13.8
Water to Land / Tidal Zone	0.0
No Change	47,006.5

Following Table 12, both mangrove reforestation and in particular regeneration show that MAR Fund's activities have led to positive developments between 2015 and 2018. The change statistics indicate an overall decrease in seagrass coverage of 94.5 hectares during this time (Table 10). This trend is primarily due to areas offshore of the Reserva Natural Tapón Creek and Río Quehueche (located just North of Livingston). It should be noted that seagrass meadows are often difficult to detect due to turbid waters and bad weather conditions, and both these areas are located directly in front of rivers whose plumes increase turbidity levels in the coastal waters. This, together with natural seasonal fluctuations in seagrass coverage, indicate that the statistics in Table 12 should be interpreted with caution. The present study corresponds an assessment at on point of time. The inter seasonal and interannual are not assessed. Sea grasses respond to natural light variations, salinity, acidity, human pressure, turbidity, marine pests and many more. The dynamic nature of seagrass meadows in response to natural environmental variation complicates the identification of changes caused by humans. The large loss of seagrass (94.5 ha) is explainable with differing image data quality and varying turbidity levels between 2015 and 2018, and has been observed for other MAR Fund study sites.

Figure 18 displays areas of land cover change between 2015 and 2018 within the Río Sarstún Multiple Use Area.

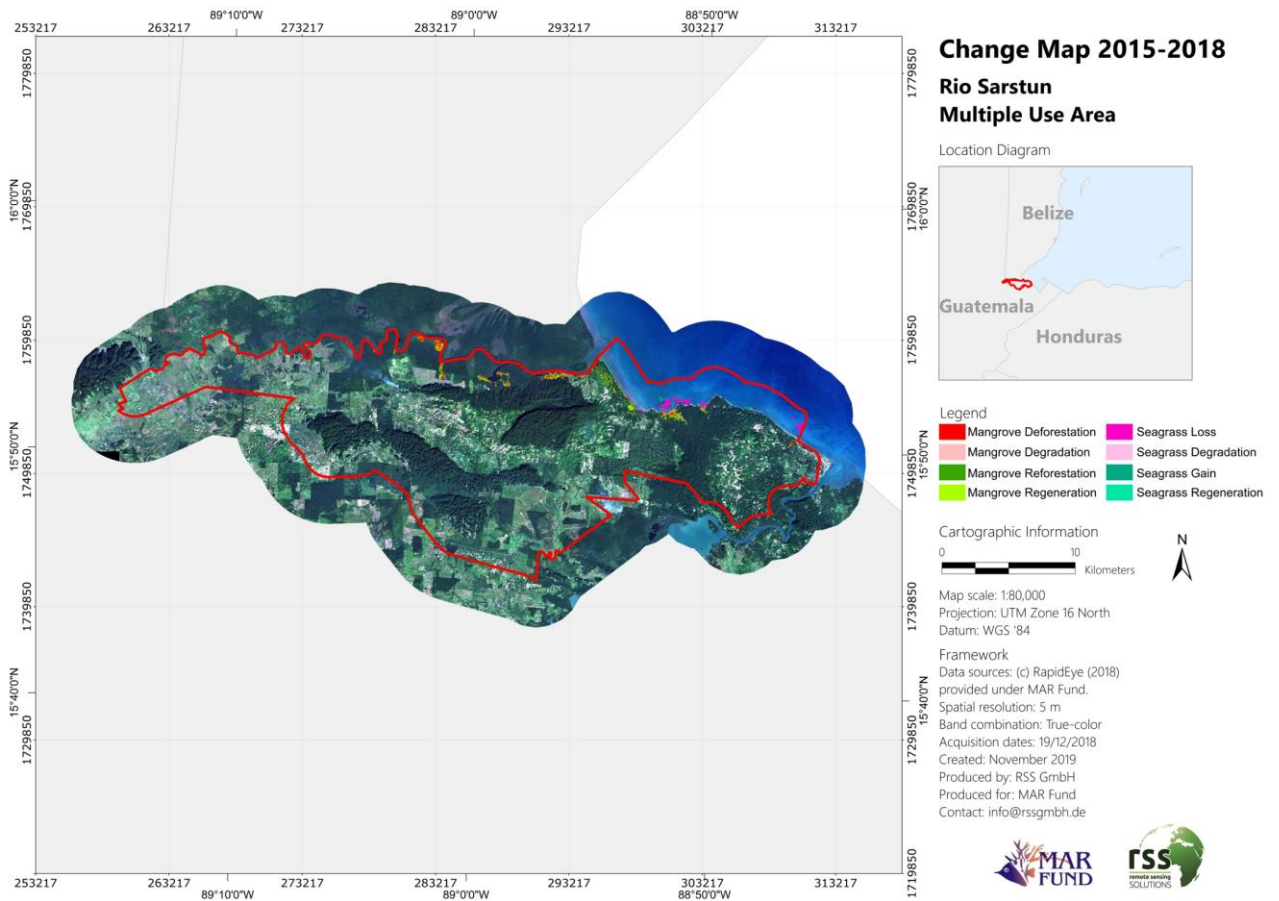


Figure 18: Land cover change map for the period between the years 2015 and 2018. In the upper right diagram, the location of the Río Sarstún Multiple Use Area within Guatemala is displayed (red).

Figure 19 displays areas of larger change within the Río Sarstún Multiple Use Area in more detail.

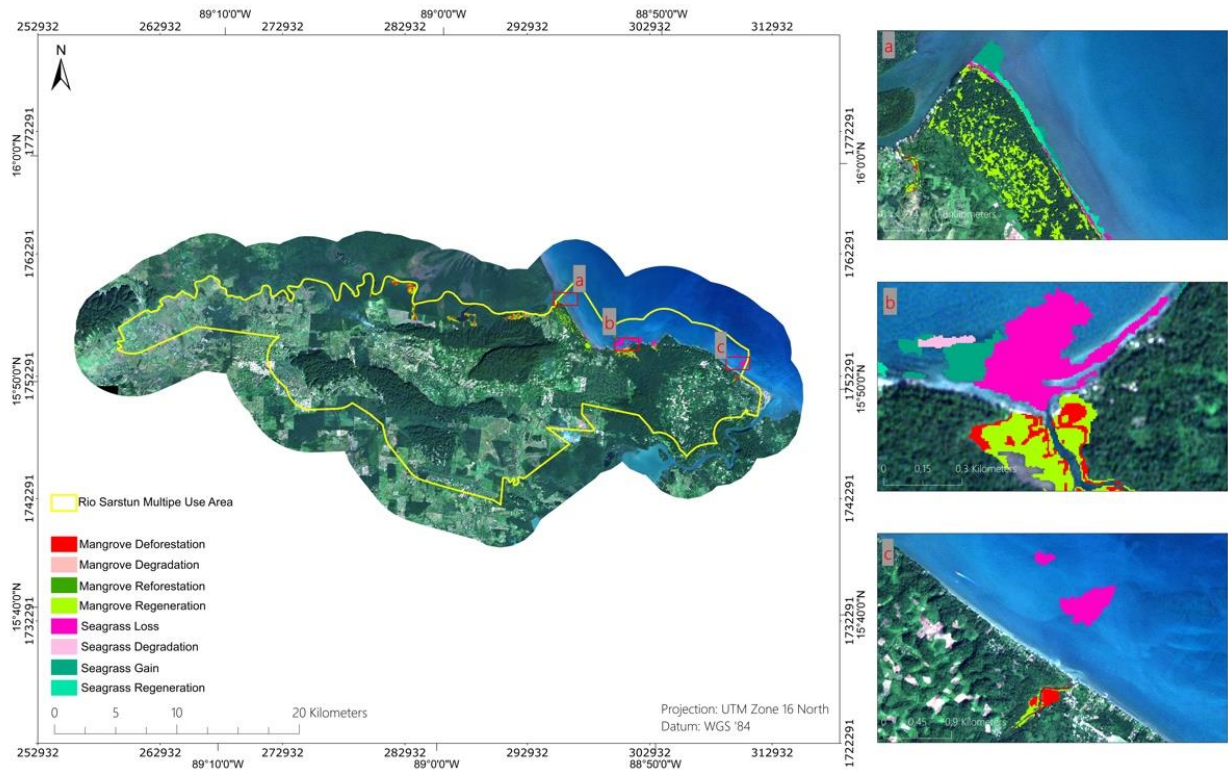


Figure 19: Examples for mangrove and seagrass changes detected between 2015 and 2018. The changes are superimposed on true-color RapidEye imagery (2018-01-09 and 2018-01-23).

Areas of mangrove regeneration are depicted in Figure 19 a & b. Very little mangrove reforestation was detected over the study area. Large seagrass areas identified as “Seagrass Loss” can be observed in Figure 19 b & c. A further analysis points the conclusion that these regions were most likely falsely classified as “Seagrass 50-100%” in 2015. In particular for the Río Sarstún area, the respective 2015 imagery was of minor quality due to difficult atmospheric conditions and high turbidity levels of the ocean. Here further ground truth data could help to stabilize results.

Figure 20 and Figure 21 show the potential impact area of future land cover change identified in the 2015 baseline report within the Río Sarstún Multiple Use Area. Mangrove coverage within this area has changed little, with many areas now achieving a higher mangrove density class. There is little evidence of negative impacts to mangrove coverage for the identified potential impact area. Greater change can be seen in the seagrass coverage class (Figure 21), with substantial losses in both density classes. One of the dominant seagrass species in the study area, *Thalassia testudinum*, is susceptible to annual die-off and may thus experience natural coverage fluctuations from year to year. Furthermore fluctuating water turbidity levels pose changing levels of difficulty in detection via remote sensing, which for this area was particularly tricky due to greatly varying image quality between 2015 and 2018.

299628







1752845

Mangrove Cover Impact Area within the Río Sarstún Multiple Use Area

Location Diagram



Legend

-  Mangrove 75-100%
-  Mangrove 50-75%
-  Mangrove 25-50%
-  Mangrove 0-25%

Cartographic Information

0 0.5 Kilometers



Map scale: 1:3,500
Projection: UTM Zone 16 North
Datum: WGS '84

Framework

Data sources: (c) RapidEye (2018)
provided under MAR Fund.
Spatial resolution: 5 m
Band combination: True-color
Acquisition date: 19/12/2018
Created: November 2019
Produced by: RSS GmbH
Produced for: MAR Fund
Contact: info@rssgmbh.de



Figure 20: Earlier identified impact area of potential land cover change within the Río Sarstún Multiple Use Area. Displayed are the four mangrove density classes (0-25%, 25-50%, 50-75%, and 75-100%). In the upper right diagram, the location of this impact area within the Río Sarstún Multiple Use Area is displayed (yellow).

299638



1752846

Seagrass Cover Impact Area within the Río Sarstún Multiple Use Area

Location Diagram



Legend

- Seagrass 50-100%
- Seagrass 20-50%
- Water (incl. 0-20% seagrass coverage)*

* also includes, besides macro-algae, algal macrophytes, algal periphyton and submerged corals, the possible occurrence of seagrasses below 20% coverage

Cartographic Information

0 0.5 Kilometers



Map scale: 1:3,500
Projection: UTM Zone 16 North
Datum: WGS '84

Framework

Data sources: (c) RapidEye (2018)
provided under MAR Fund.
Spatial resolution: 5 m
Band combination: True-color
Acquisition date: 19/12/2018
Created: November 2019
Produced by: RSS GmbH
Produced for: MAR Fund
Contact: info@rssgmbh.de



Figure 21: Earlier identified impact area of potential land cover change within the Río Sarstún Multiple Use Area. Displayed are the three aquatic classes (Water incl. 0-20% seagrass coverage, 20-50%, and 50-100% seagrass coverage). In the upper right diagram, the location of this impact area within the Río Sarstún Multiple Use Area is displayed (yellow).

6 Accuracy Assessment

An independent accuracy assessment and verification of the classification results with reference data is an essential component. The accuracy analysis provides a confusion matrix considering user and producer accuracies, the overall accuracy and the kappa index (Congalton 1991). Regarding the amount of ground truth data for this accuracy assessment, a balance between what is statistically sound and what is practicable must be found (Congalton and Green 1999). Congalton and Green (1999) propose as a "rule of thumb" to collect a minimum of 50 samples for each class in the confusion matrix. As the spatial extent of the area is medium large (47,576 ha), it was decided to use 50 samples per class. Ground truth data points were collected directly by FUNDAECO for Río Sarstún Multiple Use Area. The ground truth campaign was planned in cooperation with RSS GmbH. The field data assessment followed a strict protocol provided by RSS GmbH to assure objectivity and scientific validity. Both mangrove and seagrass cover points were requested and 3/5 (terrestrial/aquatic) of the requested 25/50 points were delivered (Figure 22). Field data coverage classes were compared with site photos from the campaign data and, for the few cases where necessary, the coverage class was changed to remain consistent with the coverage classes for all five assessed MAR Fund sites. If a particular coverage class was overrepresented in the final dataset, a set random sample of points was removed to keep validation point totals consistent across all classes.



Figure 22: Location of the 8 ground truth data points collected for the Río Sarstún Multiple Use Area by Fundaeco. Both seagrass and mangrove cover data were requested.

Large portions of the seafloor of the coastal area in Río Sarstún Multiple Use Area is predominantly covered by rocky areas, which in turn is primarily covered in "fuzzy finger" (*Dasycladus vermicularis*), other algae, and sparse seagrass. Figure 23 shows a plot with two scattered seagrass species ("turtle grass" *Thalassia testudinum* and "shoal grass" *Halodule sp.*) and the algae "fuzzy finger" (*Dasycladus vermicularis*). The spectral similarities between the two seagrass species and "fuzzy finger" may lead to misinterpretations using RapidEye imagery. The spectral and spatial resolution of the data (5 spectral bands, 5 m spatial resolution) does not allow the meaningful discrimination of these species.



Figure 23: Example of a plot with two scattered seagrass species ("turtle grass" *Thalassia testudinum* and "shoal grass" *Halodule sp.*) and the algae "fuzzy finger" (*Dasycladus vermicularis*). The spectral similarities between the two seagrass species and "fuzzy finger" can lead to misinterpretation when classified using RapidEye imagery. Especially low coverages of seagrass (<20%) within a mixed appearance of "fuzzy finger" and seagrass cannot be detected using RapidEye imagery under the given circumstances (turbidity, due to suspended matter).

As this ground truth data collection would not reach the sufficient amount of 50 points per class, an additional reinterpretation of samples from the original data (RapidEye imagery) in an independent manner is permissible in such a case (Congalton and Green 1999). A random sample of additional 392 points was selected using ArcGIS, which were afterwards interpreted by an independent remote sensing expert not involved in the classification. Random sampling reduces the risk of bias and allows for an objective assessment of the uncertainty of the estimates. Table 13 shows number of samples per class collected in the field and those collected in the original satellite imagery (RapidEye).

Table 13: Number of ground truth samples per class collected in the field and in the original RapidEye satellite imagery. The field data were collected by the local experts of Rio Sarstún, while the Ground truth data collected in the Rapid Eye imagery were collected by RSS experts. These data were assumed as 'true' in the accuracy analysis. All ground truth points were chosen randomly, to prove objective results.

Class	Collected in the field	Collected in the imagery*	Sum
Mangrove 75-100%	2	48	50
Mangrove 50-75%	0	50	50
Mangrove 25-50%	0	50	50
Mangrove 0-25%	0	50	50
Seagrass 50-100%	0	50	50
Seagrass 20-50%	0	50	50
Land/Tidal Zone	2	48	50
Water**	4	46	50
Sum	8	392	400

* Original RapidEye satellite imagery

** The class Water also includes, besides macro-algae, algal macrophytes, algal periphyton and submerged corals, the possible occurrence of seagrass below 20% coverage.

Several statistical measures for the accuracy (overall accuracy, Kappa coefficient of agreement, producer's and user's accuracy per class) were calculated. Table 14 and

Table 15 show the detailed results of the accuracy assessment. An **overall accuracy of 85.8%** with a **Kappa coefficient of 0.88** was achieved.

Table 14: Confusion matrix per class by the use of 400 reference samples. The left column shows the respective class, the row from left to right shows the classes of the classification number of reference points. Please consult Congalton (1991) or Foody (2002) for further clarification. The diagonal grey cells display the number of matching samples

Confusion Matrix		Validation class							
Classification class	Mangrove 75-100%	Mangrove 50-75%	Mangrove 25-50%	Mangrove 0-25%	Seagrass 50-100%	Seagrass 20-50%	Land/Tidal Zone	Water*	Sum
Mangrove 75-100%	44	4	2	-	-	-	-	-	50
Mangrove 50-75%	4	39	4	1	-	-	-	2	50
Mangrove 25-50%	-	-	42	6	-	-	-	2	50
Mangrove 0-25%	-	-	1	43	-	-	1	5	50
Seagrass 50-100%	-	-	-	5	44	1	-	-	50
Seagrass 20-50%	-	-	1	4	5	40	-	-	50
Land/Tidal Zone	-	-	-	-	2	-	48	-	50
Water*	1	-	2	-	-	3	1	43	50
Sum	49	43	52	59	51	44	50	52	400

*The class Water also includes, besides macro-algae, algal macrophytes, algal periphyton and submerged corals, the possible occurrence of seagrass below 20% coverage.

Table 15: Producer and user's accuracy per class

Class	Producer's Accuracy	User's Accuracy
Mangrove 75-100%	90%	88%
Mangrove 50-75%	91%	78%
Mangrove 25-50%	81%	84%
Mangrove 0-25%	73%	86%
Seagrass 50-100%	86%	88%
Seagrass 20-50%	91%	80%
Land/Tidal Zone	96%	96%
Water*	83%	86%

* The class Water also includes, besides macro-algae, algal macrophytes, algal periphyton and submerged corals, the possible occurrence of seagrass below 20% coverage.

7 Deliverables

- Original RapidEye image from 19/12/2018 (GeoTIFF)
- Original Landsat 8 image from 17/05/2018 (GeoTIFF)
- Original Sentinel-2 imagery from 01/12/2018 and 31/12/2018 (JPEG 2000)
- Preprocessed RapidEye image from 19/12/2018 (GeoTIFF), XML-Metadata
- Preprocessed Landsat 8 image from 17/05/2018 (GeoTIFF), XML-Metadata
- Preprocessed Sentinel-2 image from 01/12/2018 and 31/12/201 (Band Sequential (.bsq) image file), XML-Metadata
- Mangrove cover classification (Shapefile and Layerfile), XML-Metadata
- Seagrass cover classification (Shapefile and Layerfile), XML-Metadata
- Change 2016 – 2018 (Shapefile and Layerfile), XML-Metadata
- Mangrove map in A0 (pdf and ArcGIS .mxd-file), XML-Metadata
- Seagrass map in A0 (pdf and ArcGIS .mxd-file), XML-Metadata
- Detailed map of hot spots / heavy impact sites / touristic sites (pdf and ArcGIS .mxd-file), XML-Metadata

8 Conclusions and Recommendations

Based on comparison of the 2015 and 2018 measurements (

Table 11 and Table 12), one of the main objective indicator of the MAR Fund Phase II project were not literally achieved. In total the Mangrove areas detected, were in 2018 slightly smaller than 2015. The total area of Mangroves decreased by 3.3 ha (0.5% of the Mangrove class). However, the Mangrove regeneration within the class accounted for 385 ha, meaning that the largest part of the area is regenerating

- Areas of mangrove in project CMPA 2018 are equal to or greater than the baseline (as assessed in 2015)

We could not achieve the second main objective indicator of the MAR Fund Phase II project:

- Areas of marine seagrass beds in project CMPA 2018 are equal to or greater than the baseline (as assessed in 2015)

Change statistics (Table 12) showed an overall decrease in seagrass coverage within the study area. Seagrass loss and degradation together sum to 141 ha, as oppose to gain and regeneration, which sum to 74 ha. This is in particular due to changes in large seagrass patches located offshore of the Reserva Natural Tapón Creek and Río Quehueche (located just North of Livingston). Closer analysis of imagery from 2015 as compared to that for 2018 suggests that varying level of water turbidity and water surface induced reflectance noise and played a heavy role in this change. Smaller variations in seagrass detection between 2015 and 2018 due to differing image quality due to issues with water turbidity and meteorological conditions have been observed for other MAR Fund study sites.

Even though the absolute number of the areas show a decrease, MarFund's activities have to be considered as positive: seagrass area could not be assessed with high accuracy due to varying levels of water turbidity and water surface induced reflectance noise in the image data. The fact that the largest part of the mangrove forest are regeneration, indicates positive development.

Data from ground truth campaigns, implemented by local experts, provided an excellent basis for a realistic accuracy assessment and confirms the results of this study. To improve the outcome of the accuracy assessment activities in future projects, we continue to recommend extending local ground truth activities as much as possible under the project budget. At least 50 samples for each desired class should be collected (Congalton and Green 1999). For larger areas, i.e. in excess of 400,00 ha, at least 75 samples should be collected per desired class (Congalton and Green 1999). Acquisition of additional field data, beyond the minimum requirement for ground truthing, would allow for integrated development of the classification algorithms and potentially improve greatly the reliable assessment of object properties. Survey by drones have become more prevalent with recent technological advances, making the learning curve for implementation within field campaign activities more feasible following a short (1-2 day) training session. RSS GmbH has already had good success conducting such workshops in Indonesia for peat forest modelling activities. This would allow project partner field teams to more easily collect ground truthing data, especially in areas that are difficult or inaccessible by foot.

This study has shown that seagrass and mangrove coverage can be reliably assessed using actual high-resolution satellite imagery in good quality at low costs. RapidEye archive data costs approx.

1 € per SQKM, whereas Landsat 8 and Sentinel-2 data are free of charge. Planet Lab Inc. announced October of this year that it will continue the highly popular RESA program, which could offer an opportunity to conduct future such studies for a lower price.

With the global Corona crisis a noticeable reduction in tourism is expected, which is an important source of income for Guatemala and the countless local communities in the region. Nevertheless, the conservation and protection of the habitats must be followed from a more holistic point of view. Right now (April 2020) nobody has a reliable idea of what the future will be like, but programs like MarFund to drive regional funding and partnerships for the conservation, restoration, and sustainable use of the Mesoamerican Reef and thus support riparian states of the MAR region.

References

- Atkinson, P. M. and Lewis, P. (2000). Geostatistical classification for remote sensing: an introduction. *Computer & Geosciences* 26: 361-371.
- Ballhorn, U., Mott, C., Atwood, E. C., Siegert, F. (2016). Establishing the baseline for seagrass and mangrove area cover in five Marine and Coastal Priority Protected Areas within the Meso-American Reef area – Río Sarstún Multiple Use Area Guatemala. Final report.
- Benz, U. C., Hofmann, P., Wilhauk, G., Lingenfelder, I. and Heyen, M. (2004). Multi-resolution, object-oriented fuzzy analysis of remote sensing data for GIS-ready information. *Isprs J Photogramm* 58 (3-4): 239-258.
- Betoulle, J-L., Ramírez, S., Dubois, K. (2009). Consorcio para la Coadministración, la conservación de los recursos naturales y el desarrollo integral de los pueblos indígenas del Área Protegida “Área de Uso Múltiple Río Sarstún”. 2009. Plan Maestro 2010-2014 Área de Uso Múltiple Río Sarstún. Guatemala. 140 p.
- Chen, C. F., Son, N. T., Chang, N. B., Chen, C. R., Chang, L. Y., Valdez, M., Centeno, G., Thompson, C. A. and Aceituno, J. L. (2013). Multi-decadal mangrove forest change detection and prediction in Honduras, Central America, with Landsat imagery and a markov chain model. *Remote Sensing* 5: 6408-6426.
- Congalton, R.G. (1991). A review of assessing the accuracy of classifications of remotely sensed data. *Remote Sens Environ* 37(1): 35-46.
- Congalton, R.G. and Green, K. (1999). *Assessing the Accuracy of Remotely Sensed Data: Principles and Practices*. CRC Press, Inc., United States of America.
- Coppin P., Jonkheree, I., Nackarts, K., Muys, B. and Lambin, E. (2004). Digital change detection methods in ecosystem monitoring: A review. *Int J Remote Sens* 25(9): 1565-1596.
- Dekker, A., Brando, V., Anstee, J., Fyfe, S., Malthus, T. and Karpouzli, E. (2006). Remote Sensing of Seagrass Ecosystems: Use of Spaceborne and Airborne Sensors. *Seagrasses: Biology, Ecology and Conservation 2006*, pp. 347-359.
- Foody, G.M. (2002). Status of land cover classification accuracy assessment. *Remote Sensing of Environment* 80: 185–201.
- Green, E. P., P. J. Mumby, A. J. Edwards, C. D (2004). *Remote Sensing Handbook for Tropical Coastal Management* Clark edited by A. J. Edwards.
- Guindon, B. (1997). Computer-based aerial image understanding: A review and assessment of its applications to planimetric information extraction from very high resolution satellite images. *Canadian Journal of Remote Sensing* 23: 38-47.
- Guindon, B. (2000). Combining Diverse Spectral, Spatial and Contextual Attributes in Segment-Based Image Classification. ASPRS 2000 Annual Conference.
- Haralick, R. M. and Joo, H. (1986). A Context Classifier. *IEEE Transactions on Geoscience and Remote Sensing* 24: 997-1007.
- Hay, G. J., Niemann, K. O. and McLean, G. F. (1996). An object-specific image texture analysis of H-resolution forest imagery. *Remote Sensing of Environment* 55:108-122.

- Kartikayan, B., Majumder, K. L. and Dasgupta, A. R. (1995). An expert-system for land-cover classification. *IEEE Transactions on Geoscience and Remote Sensing* 33: 58-66.
- Kartikayan, B., Sarkar, A., Majumder, K. L. (1998). A segmentation approach to classification of remote sensing imagery. *International Journal of Remote Sensing* 19: 1695-1709.
- Kettig, R. L. and Landgrebe, D. A. (1976). Classification of multispectral image data by extraction and classification of homogeneous objects. *IEEE Transactions on Geoscience and Remote Sensing* 14: 19-26.
- Kuenzer, C., Bluemel, A., Gebhardt, S., Quoc, T.V. and Dech, S. (2011). Remote sensing of mangrove ecosystems: A review. *Remote Sens.* 3: 878-928.
- Macreadie, P. I., Anton, A., Raven, J. A., Beaumont, N., Connolly, R. M., Friess, D. A., Kelleway, J. J., Kennedy, H., Kuwae, T., Lavery, P. S., Lovelock, C. E., Smale, D. A., Apostolaki, E. T., Atwood, T. B., Baldock, J., Bianchi, T. S., Chmura, G. L., Eyre, B. D., Fourqurean, J. W., Hall-Spencer, J. M., Huxham, M., Hendriks, I. E., Krause-Jensen, D., Laffoley, D., Luisetti, T., Marbà, N., Masque, P., McGlathery, K. J., Magonigal, J. P., Murdiyarso, D., Russell, B. D., Santos, R., Serrano, O., Silliman, B. R., Watanabe, K. and Duarte, C. M. (2019). The future of Blue Carbon science. *Nature Communications* 10, 3998; doi: 10.1038/s41467-019-11693-w.
- Matsuyama, T. (1987). Knowledge-based aerial image understanding systems and expert systems for image-processing. *IEEE Transactions on Geoscience and Remote Sensing* 25: 305-316.
- McField, M. and Kramer P. R. (Eds.) (2007). *Healthy Reefs for Healthy People: A Guide to Indicators of Reef Health and Social Well-being in the Mesoamerican Reef Region*. Smithsonian Institution. Available online: <http://www.healthyreefs.org/cms/publications/>.
- Misvari, S. and Hashim, M. (2016). Change detection of submerged seagrass biomass in shallow coastal water. *Remote Sens.* 8: 200; doi: 10.3390/rs8030200.
- Mojica, A. M. (2015). Evaluación Rápida de la Efectividad de Manejo en las cinco Áreas Protegidas del Proyecto - FASE II. Proyecto Conservación de Recursos Marinos en Centroamérica. Fondo para el Sistema Arrecifal Mesoamericano. 243 pp. Retrieved from <https://marfund.org/en/conservation-marine-project/#ProjectDoc-PhaseII>.
- Mott, C (2005). *Objektorientierte Klassifikationsstrategien zur Erfassung der Landnutzung aus hochauflösenden Fernerkundungsdaten*. Technische Universität München. PhD-Thesis.
- Mumby, P. J., Green, E. P., Edwards, A. J. and Clark. C. D. (1997). Coral reef habitat mapping: how much detail can remote sensing provide? *Marine Biology* 130(2): 193-202.
- Mumby, P.J., Green, E.P., Edwards, A.J. and Clark, C.D. (1999). The cost-effectiveness of remote sensing for tropical coastal resources assessment and management. *Journal of Environmental Management* 55: 157-166.
- Nellemann, C., Corcoran, E., Duarte, C. M., Valdés, L., De Young, C., Fonseca, L., Grimsditch, G. (Eds). 2009. *Blue Carbon. A Rapid Response Assessment*. United Nations Environment Programme, GRID-Arendal. ISBN: 978-82-7701-060-1.
- Sosa-Escalante, J. E. (2013). Línea Base de Cobertura de Manglares y Pastos Marinos del Área de Protección de Flora y Fauna (APFF) Yum Balam, Quintana Roo, México. Centro para la Gestión de la Sustentabilidad (CEGES), Mérida, Yucatán, México.
- Wabnitz, C. C. C., Andrefouet, S., Torres-Pulliza, D., Muller-Karger, F. E. and Kramer P. A. (2007). Regional-scale seagrass habitat mapping in the Wider Caribbean Region using Landsat sensors:

Applications to Conservation and Ecology. University of British Columbia Fisheries Centre Working Paper Series. Working Paper # 2007-04. 44 pp.

Woodcock, C. E., Strahler, A. H. and Jupp, D. L. B. (1988). The use of variograms in remote sensing I: Scene models and simulated images. *Remote Sensing of Environment* 25: 323-348.

Annex I

List of abbreviations for the different spectral bands and indices used

Abbreviation	Band/Description	Spectral Range/Central Wavelength (nm) or Equation
RE_blue	RapidEye 2016 blue	440-510
RE_green	RapidEye 2016 green	520-590
RE_red	RapidEye 2016 red	630-685
RE_red_edge	RapidEye 2016 red edge	690-730
RE_nir	RapidEye 2016 near infrared	760-850
SE2_B2	Sentinel-2A Band 2 blue	490
SE2_B3	Sentinel-2A Band 3 green	560
SE2_B4	Sentinel-2A Band 4 red	665
SE2_B5	Sentinel-2A Band 5 vegetation red edge	705
SE2_B6	Sentinel-2A Band 6 vegetation red edge	740
SE2_B7	Sentinel-2A Band 7 vegetation red edge	783
SE2_B8	Sentinel-2A Band 8 near infrared	842
SE2_B8a	Sentinel-2A Band 8a vegetation red edge	865
SE2_B11	Sentinel-2A Band 11 short wavelength infrared	1,610
SE2_B12	Sentinel-2A Band 12 short wavelength infrared	2,190
RE2013_blue	RapidEye 2016 blue	440-510
RE2013_green	RapidEye 2016 green	520-590
RE2013_red	RapidEye 2016 red	630-685
RE2013_red_edge	RapidEye 2016 red edge	690-730
RE2013_nir	RapidEye 2016 near infrared	760-850
Anthocyanin_RI	RapidEye Anthocyanin Reflectance Index	$(1/[Mean\ RE_green]) / (1/[Mean\ RE_red_edge])$
Chlorophyll_Green	RapidEye Chlorophyll Green Index	$1 / ([Mean\ RE_nir] / [Mean\ RE_green])$
Cust_Brightness_RGB	RapidEye Cust Brightness RGB Index	$([Mean\ RE_blue] + [Mean\ RE_green] + [Mean\ RE_red]) / 3$
Green_Ratio	RapidEye Green Ration Index	$([Mean\ RE_green] + [Mean\ RE_blue]) / [Mean\ RE_blue]$
NDVI	RapidEye Normalized Difference Vegetation Index	$([Mean\ RE_nir] - [Mean\ RE_red]) / ([Mean\ RE_nir] + [Mean\ RE_red])$
NDWI_IR	RapidEye Normalized Difference Water Infrared Index	$([Mean\ RE_green] - [Mean\ RE_nir]) / ([Mean\ RE_green] + [Mean\ RE_nir])$
NDWI_Red_Edge	RapidEye Normalized Difference Water Red Edge Index	$([Mean\ RE_green] - [Mean\ RE_red_edge]) / ([Mean\ RE_green] + [Mean\ RE_red_edge])$

Segmentation parameters used

Edit Process ? X

Name

Automatic

15 [shape:0.5 compct.:0.5] creating L1'

Algorithm

multiresolution segmentation

Domain

pixel level

Parameter	Value
Condition	---
Map	From Parent

Loops & Cycles

Loop while something changes only

Number of cycles: 1

Algorithm Description

Apply an optimization procedure which locally minimizes the average heterogeneity of image objects for a given resolution.

Algorithm parameters

Parameter	Value
Overwrite existing level	Yes
Level Settings	
Level Name	L1
Compatibility mode	None
Segmentation Settings	
Image Layer weights	0, 0, 0, 0, 0, 1, 1, 1, 1, 1, 0, 0, 0, 0, 0, 0, 0, 0
RE2013_blue	0
RE2013_green	0
RE2013_nir	0
RE2013_red	0
RE2013_red_edge	0
RE_blue	1
RE_green	1
RE_nir	1
RE_red	1
RE_red_edge	1
SE2_B11	0
SE2_B12	0
SE2_B2	0
SE2_B3	0
SE2_B4	0
SE2_B5	0
SE2_B6	0
SE2_B7	0
SE2_B8	0
SE2_B8a	0
Thematic Layer usage	Yes, Yes
Classification_2013	Yes
Study_area	Yes
Scale parameter	15
Composition of homogeneity criterion	
Shape	0.5
Compactness	0.5

Thematic Layer usage

Thematic Layer usage flags

Execute Ok Cancel Help

Annex II

Field sheet for terrestrial sample points

LCCS Field Sampling RSS GmbH; Mangroves

Site ID:				Date: dd.mm.yyyy
				Time:
Location:				
Surveyor:	GPS coordinates (UTM or lat/lon):	GPS point Nr.:	Photo Nr.:	
			North East South West Up	

Mangrove coverage (%)	Mangrove species	Mixed w/ sedge or grass	Covered by other trees or palms
		Just y/n	Just y/n

Please assess four mangrove coverage levels

0% - 25%
 25% - 50%
 50% - 75%
 75% - 100%

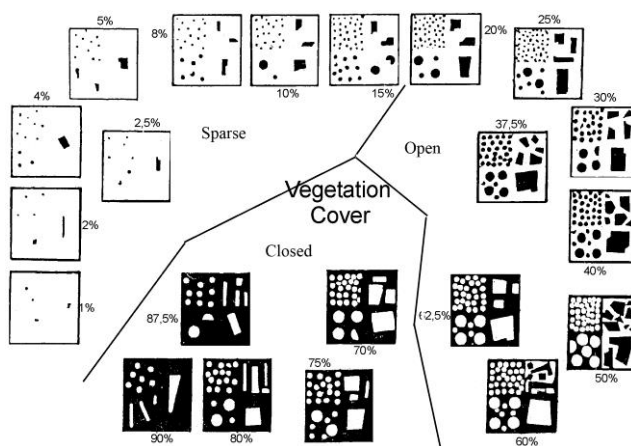
Please take 5 photos per site, standing at the GPS point

One photo facing north, one facing east, south, west
 Fifth photo should be taken directly upwards (ie. pointed at the sky)

*Locations with species taller than mangroves may be unuseable for accuracy assessment.

For a suggested location with more than 75% overgrowth coverage, consider relocating measurement point.

Comments: (anthropogenic impacts, transition zone, proximity to shore, etc.)
--



Clarification:

Everything which is dark is meant to represent canopy cover. When the background is black, as in the lower quadrats, the white objects then represent gaps in the canopy. Thus dark circles+rectangles can either represent individual trees or a stand of trees that have combined closed coverage, while the white objects represent areas where there is no canopy coverage.

Field sheet for marine sample points

LCCS Field Sampling RSS GmbH; Seagrass

Site ID:		Date:	dd.mm.yyyy
Location:		Time:	
Surveyor:	GPS coordinates (UTM or lat/lon):	GPS point Nr.:	Photo Nr.:

Depth (m)	Water clarity	Bottom type	Seagrass	Seagrass coverage (%)	Algae	Overall Coverage (%)
	Such as Secchi depth	e.g. rock, sand, pebble, etc.	Just y/n		Just y/n	

Please assess four seagrass coverage levels

- 0% - 25%
- 25% - 50%
- 50% - 75%
- 75% - 100%

*Data on species level is not necessary, but you may assess it as well.

Comments: (anthropogenic impacts, near to river, plot characteristic for surroundings, etc.)
--

More information

- <http://coralhealth.spatial.hawaii.edu/research.html>
- http://gulfsoci.usgs.gov/gom_ims/sgpubs.html
- <https://en.wikipedia.org/wiki/Seagrass>

Seagrass Percentage Cover

